UNIVERSITY OF CALIFORNIA, IRVINE

Investigating Boundary Layer Flashback of a High Turbulence Intensity Jet Flame at Gas Turbine Conditions

Thesis

Submitted in partial satisfaction of the requirements

for the degree of

MASTER OF SCIENCE

in Mechanical and Aerospace Engineering

By

Nicolas Auwaijan

Thesis Committee:

Professor G. Scott Samuelsen, Chair

Professor Vincent McDonell

Professor Tim Rupert

DEDICATION

I dedicate this thesis to my loving family whom has always been there for me.

TABLE OF CONTENTS

Page

LIST OF FIGURES

NOMENCLATURE AND SYMBOLS

Latin Symbols

Da	Damköhler number
f	Darcy friction factor
g	Velocity gradient
g_c	Critical velocity gradient
Le	Lewis number
P_0	Reference pressure, 1 atm
P_u	Ambient pressure
Pe	Peclet number
Pr	Prandtl number
Re	Reynolds number
Re_τ	Friction Reynolds number
S_f	Laminar flame velocity profile
S_L	Laminar flame speed
T_0	Reference temperature, 300 K
T_u	Unburned reactants temperature

u_τ	Shear velocity
$\bar{U}$	Mean axial velocity
$\bar{U}_f$	Mean flashback velocity
y^+	Wall units

Greek Symbols

α	Thermal conductivity
δ	Flame thickness
δ_p	Penetration distance
δ_q	Quenching distance
μ_u	Unburned reactants viscosity
τ_w	Wall shear stress
ϕ	Equivalence ratio
ϕ_f	Equivalence ratio at flashback

Acronyms

BR	Blockage Ratio
CFD	Computational Fluid Dynamics
CIVB	Combustion Induced Vortex Breakdown

DNS	Direct Numerical Simulation
LDV	Laser Doppler Velocimetry
LES	Large Eddy Simulation
NG	Natural Gas
RANS	Reynolds-Averaged Navier–Stokes
PIV	Particle Image Velocimetry
LIF	Laser Induced Fluorescence
PLIF	Planar Laser-Induced Fluorescence

ACKNOWLEDGMENTS

I would like to thank both my advisors Professor G. Scott Samuelsen and Professor Vincent McDonell for giving me the opportunity to join the UCI Combustion Laboratory as part of the Advanced Power and Energy Program. Both have provided exceptional guidance and an adequate place to learn and grow as both a researcher and an individual.

This work was sponsored in part by the Bavarian California Technology (BaCaTEC) program. The assistance of Mr. Trent Russell and Mr. Max Venaas in the setup of the experiments and collection of the data is acknowledged.

ABSTRACT OF THE THESIS

Investigating Boundary Layer Flashback of a High Turbulence Intensity Jet Flame at Gas Turbine Conditions

By

Nicolas Auwaijan

Master of Science in Mechanical and Aerospace Engineering

University of California, Irvine, 2019

Professor G. Scott Samuelsen, Chair

Hydrogen derived from non-fossil sources is an attractive candidate to replace carbon based fuels in gas turbines, as it is inherently carbon free. Yet the unusual combustion properties of hydrogen requires some care to successfully use it in gas turbines. To attain the lowest NO_x emissions, uniformly low reaction temperatures must be assured thus the reactants must be well mixed. This is accomplished in low emission gas turbines by mixing the reactants within a pre-mixer section prior to entry into the combustor. With the addition of hydrogen into the fuel, certain issues arise such as higher flame speeds compared to carbon based fuels. Flashback is a phenomena that occurs when the flame no longer propagates downstream of the injector but instead retracts and propagates upstream towards the pre-mixer and injector. Flashback occurs when the flame speed exceeds the local flow velocity. In the present work, studies are conducted under different levels of turbulence intensity. Higher turbulence intensity is known to increase

turbulent burning velocity, hence the question of how flashback propensity is affected is raised. Studies are conducted at pressures from 3 to 8 atm. with preheated reactants up to 750 K utilizing hydrogen as the fuel. The results show that even with significantly different turbulence intensities (ratio of flow centerline turbulence to centerline axial velocity) boundary layer flashback is not strongly affected. This is attributed to the role of the quenching distance in connection with the boundary layer. Core flow flashback or other flashback mechanisms may be affected differently.

1. Introduction

1.1. Overview

As operators of gas turbines move towards lower emissions and carbon free fuels, new research must be conducted to allow for safe and efficient operation of the machinery. Hydrogen derived from non-fossil sources is an attractive candidate as it is inherently carbon free. Yet the unusual combustion properties of hydrogen require some care to successfully use it in gas turbines. Gas turbine engineers must deal with four main operability issues when implementing and/or adding alternative fuels in the gas turbine: lean blow-off, auto ignition, flashback, and dynamic stability [1]. Typical gas turbines operate near lean blow-off conditions (i.e., low equivalence ratios) to reduce combustion temperatures and therefore reduce temperature dependent formation of unwanted pollutants such as NOx. To attain the lowest NOx emissions, uniformly low reaction temperatures must be assured and thus the reactants must be well mixed. This is accomplished in low emission gas turbines by mixing the reactants within a premixer section prior to entry into the combustor [2]. With the addition of hydrogen into the fuel, certain issues arise such as higher flame speeds compared to carbon-based fuels at a given equivalence ratio and flame temperature. Flashback is a phenomena that occurs when the flame no longer propagates downstream of the injector but instead retracts and propagates upstream towards the pre-mixer and injector causing significant damage in equipment as these parts are not meant to undergo such high temperatures [1,3]. Flashback occurs when the flame speed exceeds either the local or bulk flow velocity. Flashback is categorized in four distinct categories: core flow, flame instabilities, induced vortices, and boundary layer flashback (BLF). Typical gas turbines operate with certain combustor pressure drop in order to attain good mixing and stable combustion.

These pressure drops generally preclude core flow flashback if the premixer is well designed and free from large separation regions. However, even with a well-designed premixer, BLF is the most prominent form of flashback to occur as the bulk velocity near the injector wall is close to zero and it is more likely that the flame speed propagates faster than the fuel/air mixture. The critical point where flame speed is equal to bulk flow velocity is known as the penetration distance δ_p. The quench distance δ_q is the minimum distance from a wall where a flame can exist. The quench distance is crucial as it is the point where BLF occurs. Gas turbines that operate with high hydrogen content fuels are especially prone to flashback due to high flame speed and small quenching distance associated with these fuels.

A past study on the effects of turbulence intensity on turbulent flame speed was addressed by Driscoll et al. [97] where a relationship was developed stating that turbulent flame speed increases as a function of turbulence intensity. Since the local turbulent flame speed is highly dependent on turbulence intensity, the value of turbulence intensity must be measured at the point of interest since pressure fluctuations can cause a decay in the flow field as it moves downstream. Four definitions of turbulent flame speed exist because of sensitivity of factors on its response and each serve a purpose based on experimental setup. The four turbulent flame speed definitions are local displacement speed, global displacement speed, local consumption speed, and global consumption speed. The local displacement speed serves a purpose where the propagating velocity of the flame brush with respect to the frame of reference is stationary, such that applications of burners that create detached locally normal flames can be accessed with little uncertainty (i.e. no flame holder/edge) [102]. The global displacement speed is the average of the local displacement speed over the entirety of the turbulent flame brush. The local and global consumption speed are the opposite of the displacement speeds mentioned. The local

consumption rate does not require a mean flame surface. Driscoll et al. [101] states that the significance of local consumption speed is to provide quantitative features of premised turbulent flames for validating models and simulations, hence this method is used in this work.

The flashback mechanism discussed later in this thesis indicated that when the local turbulent flame speed exceeds the local fuel-air mixture velocity flashback occurs. No prior experimental study observing the effects of turbulence intensity on flashback propensity has been observed, thus it is important to develop as industry is moving towards higher turbulence intensity in the premixer to reduce emissions. To address this gap in knowledge, the objective of the present work is to obtain new experimental data in which turbulence levels of the reactants are varied and the impact of this on flashback propensity evaluated.

1.2. Goal

The goal of the work provided in this paper is to observe the effects of bulk flow turbulent intensity on boundary layer flashback of a jet flame at gas turbine conditions (i.e., non-confined flame, high pressure, jet flame, and high temperature).

1.3. Objectives

To address this gap in knowledge, the objectives of the present work are:

1. Develop a means to control turbulence intensity.
    - Design and test a perforated plate that is capable of increasing turbulence intensity based off a backflow ratio using LDV
2. Conduct experiments.
    - Test the turbulence intensity setup experimentally at gas turbine conditions and measure the flashback propensity

3. Evaluate the critical velocity gradient at flashback.
    - Utilizing CFD, ANSYS® FLUENT, to capture the velocity gradient value at the quench distance of the non-fully developed turbulent flow at flashback conditions
4. Analyze the CFD velocity gradient
    - Compare the Blasius velocity gradient to the value extracted using CFD at the quench distance.

2.0 Background

Combustion of carbon-based fuels (fossil fuels), currently and in the future will continue to, play an important role in the power generation sector. Main fossil fuels consumed in industry are petroleum and natural gas, which are essential for safe and reliable power generation worldwide. Carbon based combustion driven engines provide consistent reliability and the capability to exceptionally load follow [1,4]. Due to the benefits of gas turbines, as commercial used power generators, industry and researchers have been working to further improve combustion efficiency as well to allow for fuel variability [1,5]. As the performance of gas turbines have evolved over time, a key concern that remains are associated with the emitted pollutants. Environmental awareness has prompted development of combustion systems with remarkably low pollutant emission levels [6,7]. To accomplish this task, the temperature inside the combustor is strictly controlled and a premixer is utilized [1,5,8]. The premixer allows for the fuel and air to mix as uniformly as possible before ignited to avoid pockets of rich/lean zones. Also, gas turbines operate at low enough combustion temperatures to avoid thermal NO_x but faces the issue of lean blow-off in return. Operability issues of premixed flames in gas turbines include lean blow-off, auto-ignition, flashback, and dynamic stability [1,5,8]. To avoid these operability issues gas turbines, operate in small regimes of fuel/air ratio. Due to this, development of gas turbines is designed beforehand for its desired application and fuel variations. The mentioned operability issues can cause damage to the engine. The stability of the combustion system has been extensively studied in past few decades to address this problem [8,9]. Since the ability of extracting natural gas using advanced hydraulic fracturing technology, the consumption of this fuel has risen [10,11]. Also, due to the low carbon-to-hydrogen ratio and low emission nature of Natural gas compared to solid and liquid alternatives, the appeal of the fuel seems more

favorable. However, the combustion of all fossil derived hydrocarbons generates pollutants including CO, unburned hydrocarbons (UHC), particular matter (C), and CO_2, which is a greenhouse gas produced from the combustion of the fuel. As cleaner sources of fuel (i.e. low or no carbon-based fuels) are the outlook to reduced greenhouse gasses, strategies to replace natural gas with renewable sources (e.g., alternative fuels) are pursued [12]. Alternative fuels, such as hydrogen, play an important role in eliminating the direct generation of greenhouse gasses. Steam reforming of natural gas is a common method of hydrogen production [13,14] in which hydrogen based fuels can be derived while allowing the suppression of the associated carbon [15]. Integrated gasification combined cycle (IGCC) represents a clean technology to manage CO_2 emission from coal [16,17]. The synthesis gas produced through the process of IGCC constitutes hydrogen and carbon monoxide as the main produce and can be further shifted to H_2 and CO_2 through water reactions [15]. The captured CO_2 can afterwards be sequestered, which is the process of storing the product, thus reducing greenhouse emission and mitigating climate change [18,19]. Hydrogen can also be produced renewably via electrolysis of water using electricity generated by wind or photovoltaic [20]. This hydrogen can be used in addition to the existing natural gas infrastructure or combusted directly.

Alternative fuels and premixer conditions will play an increasingly important role for carbon and pollutant mitigation in gas turbine systems. This brings about the importance of high hydrogen content fuels [21] for which the fuel/air mixture preparation and combustion behavior needs to be investigated and understood. Another method to reduce pollutant emissions are to operate at high turbulence intensities in the premixer to promote proper mixing. A major relevance of lean, and highly turbulent, premixed combustion systems for gas turbines is the effect of fuel composition coupled with high turbulence intensity values on flashback.

While increasing studies on flashback have appeared in the past few decades, studies of the effect of turbulence on boundary layer flashback are absent. The next sections discuss past studies ranging from simulation work to experimental work of both laminar and turbulent flames. The past work shows that there are gaps in knowledge associated with different mechanisms and their apparent effect on boundary layer flashback. The work in the paper will address knowledge gaps and add value to the background and future studies.

2.1.1 Flashback Mechanisms

Flashback is induced when the flame propagates from the combustion zone into the premixer section of the combustor. The increased temperature inside the premixer due to flashback causes components to melt and fail as they are not intended nor designed to undergo these conditions. Four mechanisms are associated with flashback in gas turbines [6,22,23]: core flow flashback, combustion instability induced flashback, combustion induced vortex breakdown (CIVB), and boundary layer flashback.

2.1.2 Core Flow Flashback

Core Flow Flashback Flame propagation in the core flow occurs when the turbulent burning velocity exceeds the local flow velocity in the core flow [8,22]. Core flow flashback is a function of turbulent-flame interaction as well as chemical kinetics [24]. Fuel composition and the turbulent flame structure are parameters for determining core flow flashback limits [25,26]. Core flow flashback is easily avoided by increasing the axial velocity. With the introduction of swirled flames, the axial velocity decreases as some momentum of it shifts to radial, which can lead to flame stretching due to the vortex-flame interaction as it increases the turbulent flame speed [27,28,29].

Turbulent burning velocity, which has been extensively studied in the literature, is typically represented as a function of laminar flame speed and turbulence attributes [30,31,32,33]. Hydrogen having higher flame speeds compared to carbon bases fuels at a given condition accelerates flashback propensity. Turbulent burning velocity correlations have been used as a tool to predict flashback [24,34].

2.1.3 Combustion Induced Instability Flashback

Combustion induced instability flashback occurs due to large amplitude fluctuations in the flow field [8,23]. These instabilities are generated by interactions of acoustic modes, unsteady heat release, and flow structure. Flame lifting can occur due to pulsations in the flow field, which leads to the flame lifting off an edge and inducing flashback. Combustion induced instability flashback was observed by Thibaut et al. [23] using a large eddy simulation (LES). The results captured by the LES simulation can be seen in Figure 1.

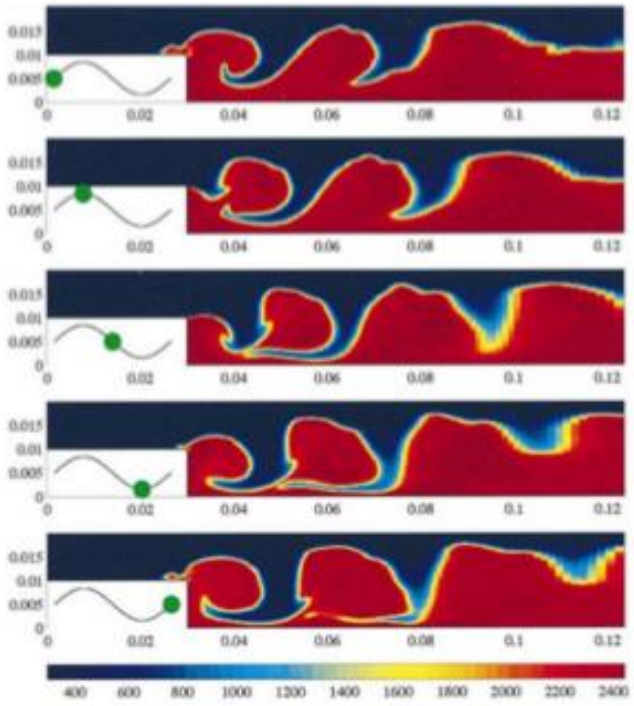

Figure 1: Premixed flame temperature distribution structure of a backward-facing step captured by an LES simulation [23]

2.1.4 Combustion Induced Vortex Breakdown

Combustion induced vortex breakdown (CIVB) flashback is prominent in swirled flames. If the swirl number exceeds a critical value, then generation of vortex breakdown occurs [35,36]. When there is a reverse flow region an increase in azimuthal velocity to axial velocity is observed. A study by Konle et al. [37], using particle image velocimetry (PIV)-laser induced fluorescence (LIF) measurements with a high temporal resolution shows a formation of a bubble at the tip within the recirculation zone, which can be seen in Figure *2*. Baroclinic torque constructs a negative vorticity, thus increasing the negative axial velocity, which in turn causes the upstream propagation of the bubble [38,39,40,41].

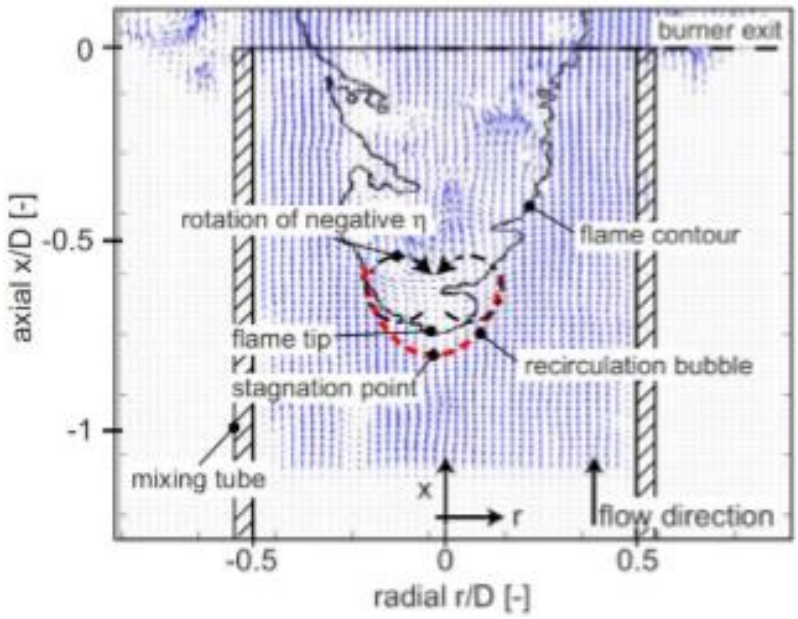

Figure 2: The instantaneous flame front relative to the recirculation bubble studied by Konle et al. [37,42].

2.1.5 Boundary Layer Flashback

Boundary layer flashback is the dominant flashback mechanism in jet flames, which can subsequently be said the same goes for gas turbine combustors [91]. Typically, at operating conditions of a gas turbines premixer the flow velocity exceed the turbulent flame speed; thus, core flow flashback is mitigated. The flow velocity near the premixer wall decreases due to the no-slip condition, thus the potential that boundary layer flashback occurs increases. The burning velocity also decreases near quenching distance, which is where the reaction cannot sustain itself due to a large amount of heat loss or flame stretch [43,44,45]. Flashback occurs near the wall where the local burning velocity can overcome the local flow velocity. Boundary layer flashback has been characterized by the "critical velocity gradient" concept in the literature [46]. The critical velocity gradient corresponds to the bulk flow velocity at the condition of flashback and

is an indicator of the flashback propensity for a given condition. Boundary layer flashback has been studied under laminar and turbulent flow conditions for different parameters including fuel/oxidizer composition, preheat temperature, operating pressure, burner material, and geometrical burner configuration with the recent research focusing on high hydrogen content fuels.

Since boundary layer flashback is the most prominent form of flashback in gas turbine application, the work provided here will focus on boundary layer flashback as the flashback mechanism.

2.2 Beginning Studies on Boundary Layer Flashback

The number of studies from 1943 to 2017 that incorporate boundary layer flashback in premixed jet flames are displayed below in Figure 3.

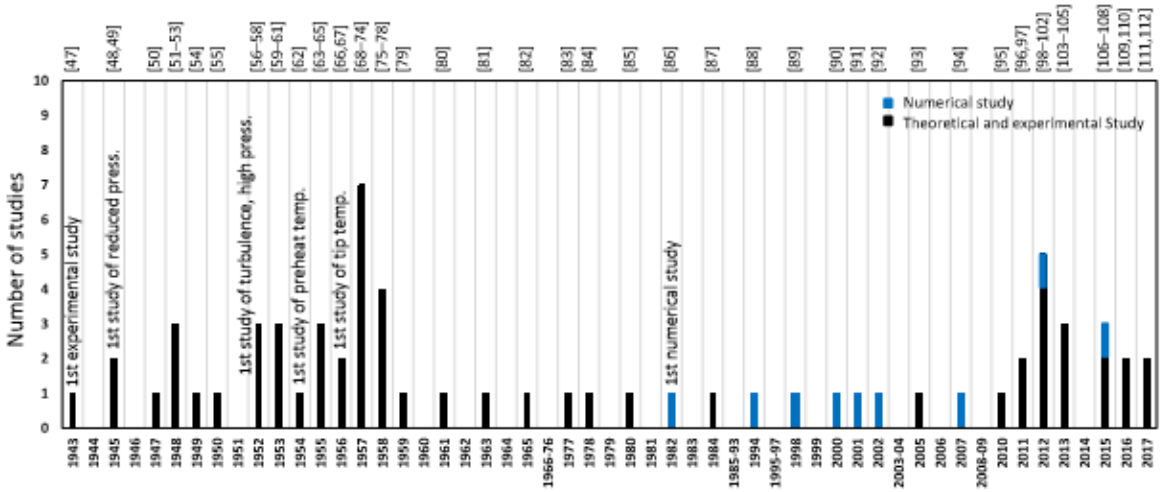

Figure 3: Amount of Studies on Boundary Layer Flashback [91]

The first systematic experiment was done by Lewis and Von whom also constructed a boundary layer flashback prediction model [46]. The first sub-atmospheric condition flashback

experiment was conducted by Garside et al. [48]. The first turbulent and high pressure flashback study was done by Edse [49], while the effect of preheat and tip temperature were first achieved by Grumer and Harris [50] and Bollinger and Edse [51], respectively. Lee and T'ien [52] first conducted a numerical study on the propagation of a premixed laminar flame inside a tube.

The study of turbulence intensity on flame speed was investigated by Driscoll et al. [97] where it is concluded that higher turbulence intensity relates to higher turbulent flame speeds. It is known that the higher the turbulent flame speed the greater the flashback propensity. A Prediction model for boundary layer flashback of multiple parameters such as fuel composition, burner material, pre-heat temperature, operating pressure, and bulk flow velocity has been developed using the Blasius profile; though the effects of turbulence intensity has not been studied before on BLF.

2.3 Basic Prediction Model for Boundary Layer Flashback

Figure 4 depicts a laminar flow moving left-to-right and encountering the flame front. The velocity profile of the fuel-air mixture is denoted as (y) and the flame speed is denoted as (y). The fuel-air mixture decreases in velocity close to the wall due to the no-slip condition. δq represent the quench distance which is where the flame is non-existing near the wall. This happens at a certain distance from the wall and part of the flame close to the wall trails behind the central position as indicated [46,47,53]. δp represents the penetration distance, which is the critical point where local flow velocity is equal to the burning velocity [54].

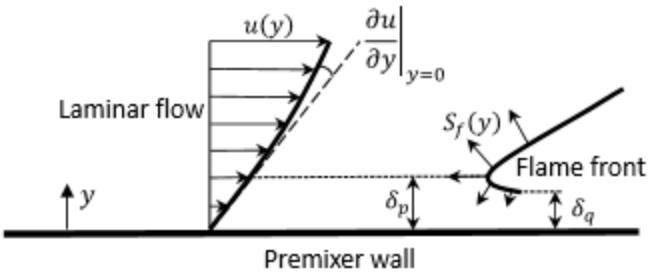

Figure 4: Critical velocity gradient prediction model schematic

The velocity gradient g has been used in literature to describe flashback at the wall. Eq. 2.1 represents this velocity gradient in terms of τ_w, the shear stress, and μ_u is the viscosity of the unburnt mixture. In literature, flashback occurs when the local fuel-air velocity drops below the burning velocity, which is typically close to the wall. The fuel-air bulk velocity magnitude at the onset of flashback is stated as the critical velocity gradient, gc. This precludes that the flame does not propagate if the velocity gradient is higher than this critical velocity gradient.

$$\mathrm{g} = \left|\frac{\partial \mathrm{u}}{\partial \mathrm{y}}\right| = \left|\frac{\tau_w}{\mu_u}\right| \qquad \text{Eq. 2.1}$$

The velocity gradient is approximated by the ratio of the unburnt fuel-air velocity to the penetration distance at the wall and shown in Eq. 2.2. This equation assumes that the unburnt fuel-air velocity stays linear near the wall.

$$g_c = \frac{u_{|y=\delta_p}}{\delta_p} \qquad \text{Eq. 2.2}$$

The critical velocity gradient can be expressed as the laminar flame speed divided by the penetration distance as stated in Eq. 2.3

$$g_c = \frac{S_L}{\delta_p} \quad \text{Eq. 2.3}$$

A fully developed laminar pipe flow with a radius of R, the velocity field can be described by Eq. 2.4

$$u(r) = 2\overline{U}\,(1 - (\frac{r}{R})^2) \quad \text{Eq. 2.4}$$

where r is radial distance and $\overline{U}$ is the bulk flow velocity. Combining Eq. 2.3 with the derivative of Eq. 2.4 at the tube wall ($r = R$), Eq. 2.5 is obtained at flashback condition (also, [57]):

$$gc = \frac{S_L}{\delta_p} = 4\frac{\overline{U}}{R} \quad \text{Eq. 2.5}$$

The critical velocity gradient developed from literature is still used today to help determine and characterize boundary layer flashback.

The previous equations were in reference to flashback prediction of laminar flames [46]. For turbulent fully developed flow in a smooth pipe, the Blasius equation is used to approximate the velocity gradient with diameter of D and a given Reynolds number Re [55]:

$$g = \frac{1}{8}\frac{f\overline{U}}{\nu} \quad \text{Eq. 2.6}$$

$$f = \frac{0.3164}{Re^{0.25}}, \; 4 \times 10^3 < Re < 10^5 \quad \text{Eq. 2.7}$$

$$g = 0.03955\, Re^{0.75}\frac{\overline{U}}{D} \quad \text{Eq. 2.8}$$

in which f and ν are friction factor and kinematic viscosity, respectively. Both Eq. 2.3 and Eq. 2.8 can be used in conjunction to predict the flashback propensity for turbulent flames [53].

Penetration distance is approximated to be the quenching distance, as mentioned in literature [47,56,0,60,61,64,66]. There are many factors that affect flashback propensity such as fuel composition, equivalence ratio, vessel pressure, inlet temperature, material, turbulence intensity and more. Multiple studies have attempted to address this problem by investigating multiple parameters [43,68–70] and attempting to find empirical relations [71–74].

The issue with the original critical velocity gradient model is that it neglects the flame-flow interaction, which has a significant effect on flashback propensity. Also, the Blasius equation has been developed to predict a velocity gradient, but this is only for a uniform flow. Thus, a non-fully developed flow will require a different technique to capture the velocity gradient, as this work will answer how and if it is necessary.

2.4 Parameters Impacting Boundary Layer Flashback

Multiple factors flashback propensity such as the following: flow field characteristics, boundary layer heating, and operating conditions.

2.4.1 Flow Field

The flow field affects boundary layer flashback propensity due to the velocity momentum near the wall. When the velocity of the flow increases so does the local burning velocity, in order to maintain flame stabilization. The velocity profile can play a key role in terms of flashback propensity. An experimental study has shown that a non-fully developed flow actually decreases flashback propensity because of the additional shear stress, a function of the entrance length, on the wall [65] and can be seen numerically in Eq. 2.1 (Figure 4). The additional shear stress increases the velocity gradient near the flow making it more difficult for the critical velocity gradient to overcome.

Stream wise turbulence intensity is significant in determining the total turbulent kinetic energy at the near wall zone. The apogee magnitude of the near-wall zone in the stream wise turbulence intensity is proportional to the shear stress velocity (u_τ) in Eq. 2.9 and is also used as a scaling parameter [103,104]. τ_w is a function of the Reynolds number and when referring to Eq. 2.1 it is noted that τ_w is related to the critical velocity gradient. It is important to keep in mind that though this flow was non-fully developed, the turbulence intensity was not changed, thus that affect has not been realized.

$$u_\tau = \sqrt{\frac{\tau_w}{\rho}} \qquad \text{Eq. 2.9}$$

2.4.2 Reynolds Number

Once Reynolds number transition to turbulent values, a significant and complex effect of the flow field on flashback propensity occurs compared to laminar conditions [80,81]. Based on a turbulent Reynolds number, the combustion regime will dictates the flame structure and defines how the small scale eddies interact with the flame [82,83]. This states that the turbulent flame speed is a function of turbulence intensity (Eq. 2.10 & 2.11) and consequently a higher turbulence intensity can result in higher flashback propensity [24]. Turbulence intensity is defined as the ratio of fluctuating flow velocity to the mean flow velocity a function of a standard deviation (Eq. 2.12).

$$\frac{S_{T,GC}}{S_{L0}} = 1 + A_2\left(\frac{u'}{S_{L0}} * \frac{1}{\delta_{L0}}\right)^{1/2} \qquad \text{Eq. 2.10}$$

$$A_2 = 0.00077 \left[\frac{\bar{U}}{S_{L0}}\right] \left[\frac{W}{\delta_{L0}}\right]^{1/2} f(Ma) \qquad \text{Eq. 2.11}$$

Where W is the burner width, δ_{L0} is the un-stretched laminar flame thickness, S_{L0} is the un-stretched laminar burning velocity, and u' the r.m.s streamwise velocity.

$$u'_{rms} = \sqrt{(u'_{ax})^2 + (u'_{rad})^2 + (u'_{azi})^2} \qquad \text{Eq. 2.12}$$

Where the subscript "ax", "rad", and "azi" are axial, radial, and azimuthal directions, respectively.

Fuel composition plays an important role on the combustion characteristics for premixed flames. Fuel composition directly changes the chemical kinetics and that will play a direct role in the flame speed. The quench distance at the wall is also affected due to fuel composition, which in turn changes the flashback limits [47,58,59,60]. Hydrogen tends to flashback sooner due to high molecular diffusivity that pays a role in the small quenching distances and high flame speeds. The Lewis number is capable of capturing the high molecular diffusivity of hydrogen, resulting in low values found in both experimental and numerical studies [84–89]. Hydrogen having a substantial higher molecular diffusivity compared to methane means that the fuel diffuses out towards the wall (i.e. closer) and the local turbulent flame speed is associated with a lower local flow velocity, making it easier to overcome and flashback. Also, the effect of preheat temperature increases the burning velocity [90], resulting in higher flashback propensity. This is due to an increase in reaction rate with temperature and increased turbulent flame speeds. Also, noticed is the higher the operating pressure the greater the flashback propensity, thus operating at gas turbine conditions can be difficult. The effects of pressure include an increase in the reaction

rate and a reduction in the quenching distance. The magnitude of the effects of these factors can be seen in Eq. 5.1.

2.5 Summary

Much work has been conducted regarding flashback phenomena and much can be learned from it. Studies of turbulence intensity effects on flame speed have been done, but not in regards to the effect on boundary layer flashback. Also, few studies have been done on turbulent jet flames with 100% hydrogen fuel content. Conducting experiments at high pressures and temperatures, gas turbine conditions, for a jet flame will benefit present and future prediction models. Incorporating the variation of turbulence intensity, which has not been studied will enhance research done in this field [91,92]. A boundary layer flashback model correlation for gas turbine conditions has been achieved before, though the factor of turbulence intensity has not been considered. It is important to study the effect of turbulence intensity on flashback since gas turbine engineers are aiming to increase turbulence intensity to better mix the fuel-air mixture prior to combustion for reduced emissions. ANSYS® Fluent is a CFD tool that can be utilized to determine the velocity gradient of a non-fully developed, and or fully developed, flow near the wall (i.e. quench distance). The present work addresses these knowledge gaps by studying the multiple effects on boundary layer flashback of turbulent jet flames at gas turbine conditions.

3. APPROACH

3.1 TASK-1: Develop a Means to Control Turbulence Intensity

Design and test a perforated plate that is capable of increasing turbulence intensity based off a backflow ratio using LDV

Turbulence intensity is defined as the ratio of the fluctuating velocity to the mean velocity using a standard deviation. Turbulence Intensity is categorized by 3 regions: low at values below 1%, moderate from 1 to 10%, and high at values greater than 10%. Multiple ways are suggested to induce varied turbulence intensity values by implementing device such as a perforated plate, slotted disk, or a mesh [98]. Past experimental studies of premixed flames in intense isotropic turbulence was investigated by Bédat et al. [98] and implemented by Marshall et al. [100]. Using the design based off of these studies, a perforated plate was made with a specific backflow ratio in order to increase the turbulence intensity of the original jet flame work at high pressure and temperature conditions by Kalantari et al. [96] by approximately 2.5 times. Based on the comparison and fact that Marshall's work verified performance at elevated pressure, it can be stated, confidently, that the produced turbulence intensity stays true at the gas turbine conditions tested in this work.

Results are to be captured by LDV.

3.2 TASK-2: Conduct Experiments

Test the turbulence intensity setup experimentally at gas turbine conditions and measure the flashback propensity

Utilizing a high pressure and temperature vessel (Figure 5), to simulate gas turbine conditions, the premixer design will be tested for flashback propensity. The facility is capable of heating 2 lb/s of air up to 1000°F. The air-fuel mixture is premixed through a long pipe before coming into contact with a turbulence intensity generator 3.4" from the burner rim. The velocity field was simulated through CFD and experimentally investigated through the use of LDV.

Thermocouples were placed at the burner rim to monitor tip temperature and a pressure transducer utilized to monitor pressure spikes in the premixer at flashback conditions. The spike in pressure is an indicator/trace used to find the data when flashback occurred. A spark ignitor was used with hydrogen as the pilot fuel to stabilize the jet flame. A camera was used to monitor the physical flame and flashback phenomena.

Two tests were conducted, the first was with no turbulence intensity generator (5.4% core turbulence intensity) and the second was with a turbulence intensity generator with an 81% blockage ratio to raise the turbulence intensity from 5.4 to 15.7%.

3.3 TASK-3: Utilize CFD to Obtain the Critical Velocity Gradient at Flashback

Obtain the velocity gradient of a non-fully developed turbulent flow at flashback conditions using CFD, ANSYS® FLUENT

Utilizing ANSYS® FLUENT as a CFD software the 3D premixer design was simulated to obtain the velocity gradient at the quench distance. The mesh was refined to resolve the boundary layer (i.e. y+ less than or equal to 1) and maximum skewness maintained below 0.9 as

the main simulation criteria. K-ε viscous model was used with a realizable enhanced wall treatment, to capture the effects near the wall with more precision (i.e. different damping coefficients) and keep computational time to a minimum solving the mesh cells near the center of the flow.

The addition of fuel was not added to the simulation to reduce computational time and since the air flow is 99% of the flow overall fuel-air flow.

3.4 TASK-4: Analysis of Velocity Gradient at Flashback Conditions

Analyze the velocity gradient of a non-fully developed turbulent flow at flashback conditions using CFD, ANSYS® FLUENT

The quench distance, approximately the penetration distance, was used as the location from the wall to obtain the velocity gradient since it is the zone of lowest local flow velocity. The value obtained via CFD for the 5.4% turbulence intensity case was initially compared to that of the gradient from the fully developed Blasius equation (eq. 2.6-2.8) since they should be similar. The values were within a 1% discrepancy of each other when the boundary layer was resolved and greater than a 100% difference when using no inflation to resolve the boundary layer. The 15.7% turbulence intensity case was then compared in similar fashion and results followed a similar trend.

4. Methods

4.1 High Pressure and Temperature Test Rig

The high pressure and temperature test rig utilized at UCI can be seen in Figure 5 along with a broad image of the premixer design that will be discussed later in this paper. A similar facility was utilized by Kalantari et al. [67].

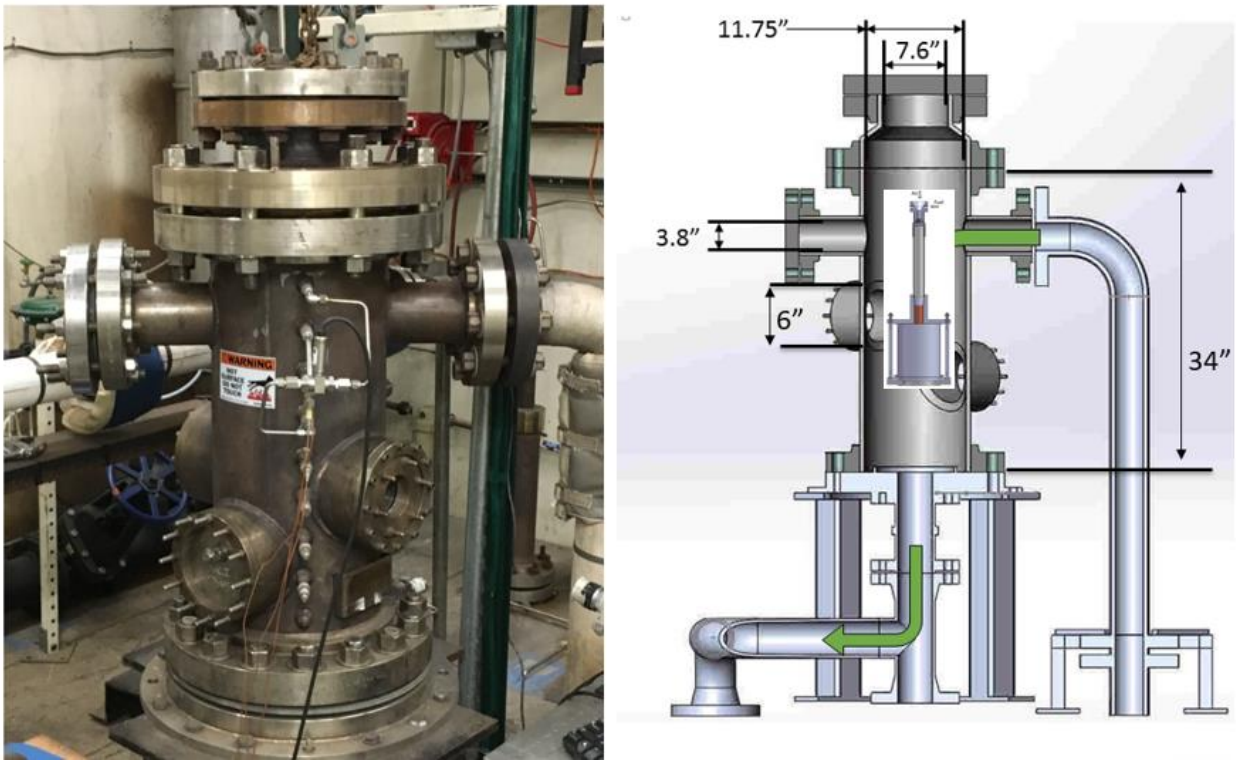

Figure 5: High pressure and temperature test rig

The UCI high pressure and temperature test rig utilizes 3 heaters in parallel to heat incoming air to desired temperatures. The air factory can flow up to 4 lb/s of air at 10 atm with 2.5 lb/s of air utilized for combustion. The air circuit can be seen in Figure 6.

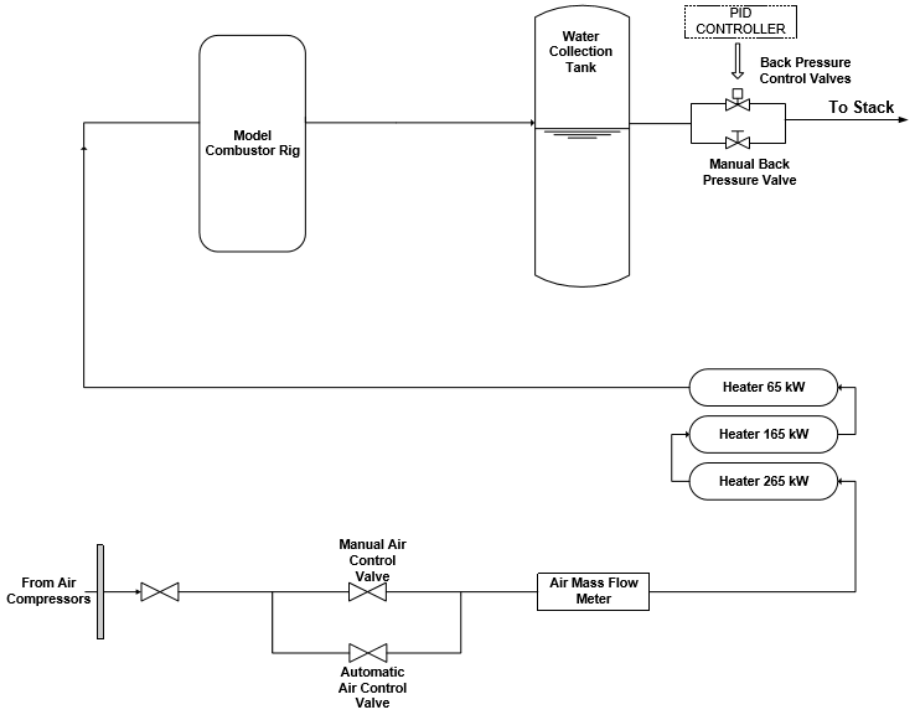

Figure 6: Air circuit

Air can be preheated up to 1000°F at 2 lb/s by the 550 kW non-vitiated heaters, though the temperature is flow dependent.

The remaining air/products from the exit of the rig is cooled before meeting the pressure bypass valve, which is used to adjust pressure in the rig. This is done by a closed water quench system (Figure 7).

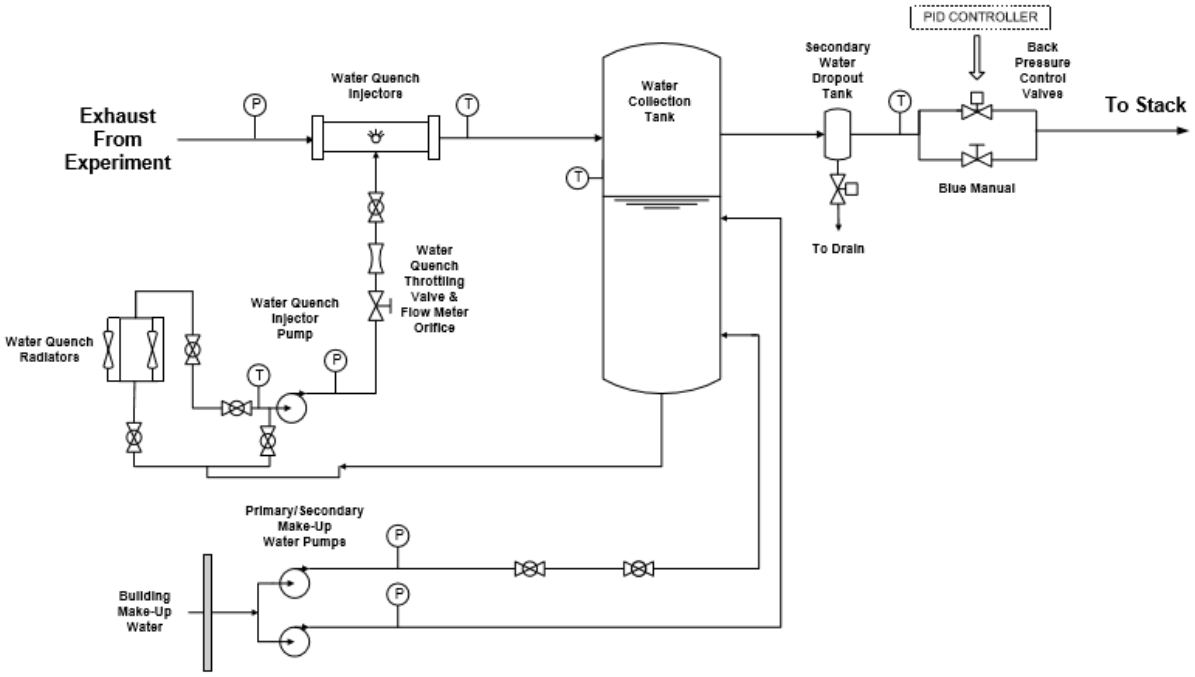

Figure 7: Closed water quench system

The fuel injection is monitored by a Micromotion CMF025 Coriolis meter that has an uncertainty of 0.5%. This is used along with other software-controlled hardware to monitor flow and equivalence ratio. Fuel can either be injected through bottles or from utilizing the UCI natural gas line. The fuel circuit schematic is displayed in Figure 8.

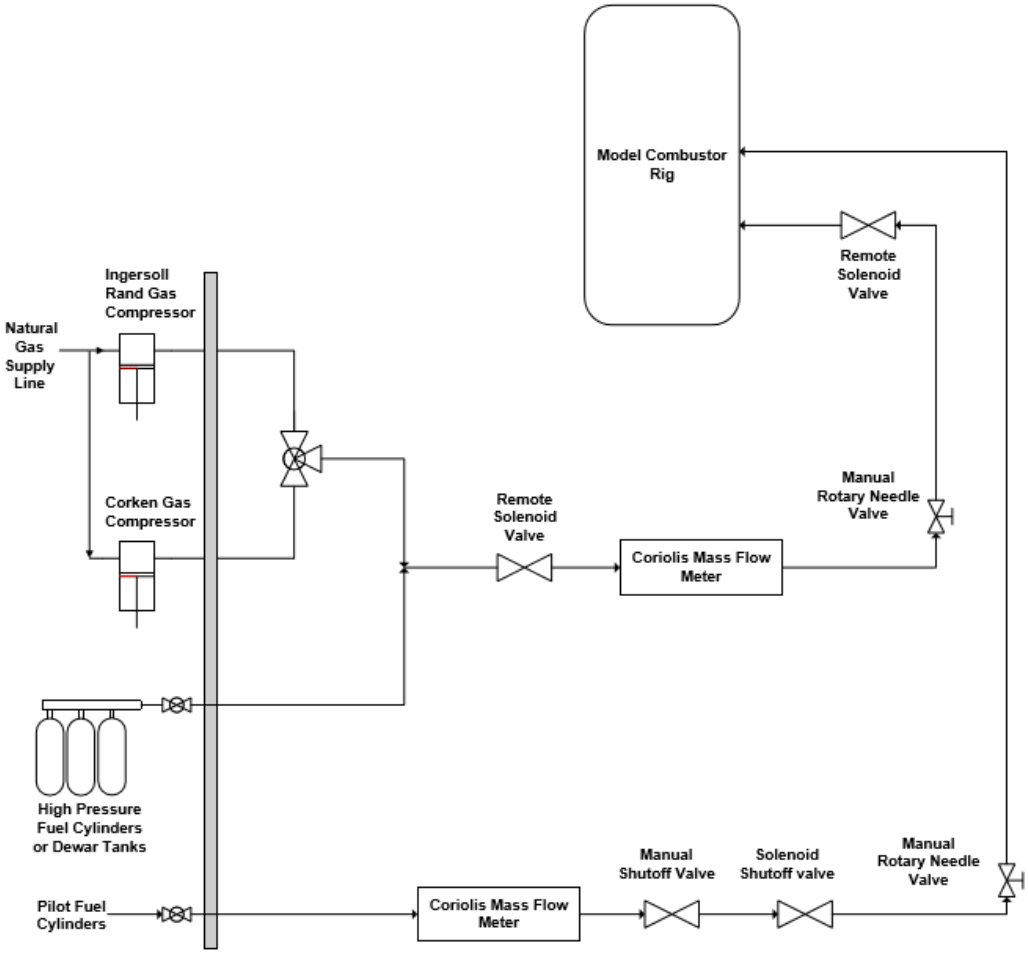

Figure 8: Fuel Circuit

Flashback data is recorded via the software LabVIEW that is connected to a data acquisition box through a National Instrument PCI board. The sensors utilized and data recorded include the inlet air temperature, burner rim temperatures, vessel pressure, differential pressure (between premixer and combustor), and air and fuel mass flow rates. The calculated properties include the equivalence ratio and bulk flow velocity.

Video was captured using a Hitachi® camera, which was used to visually monitor flashback allowing the operator to take precaution and shut-off the fuel immediately to mitigate

the flame front from damaging internal (premixer) components. Figure 9 below represents a stabilized jet flame that anchors to the burner rim while Figure 10 is the flame retracting back into the premixer (i.e. flashback). Carbon Monoxide was added to the hydrogen fuel (50/50 by volume) in these images for visual clarity.

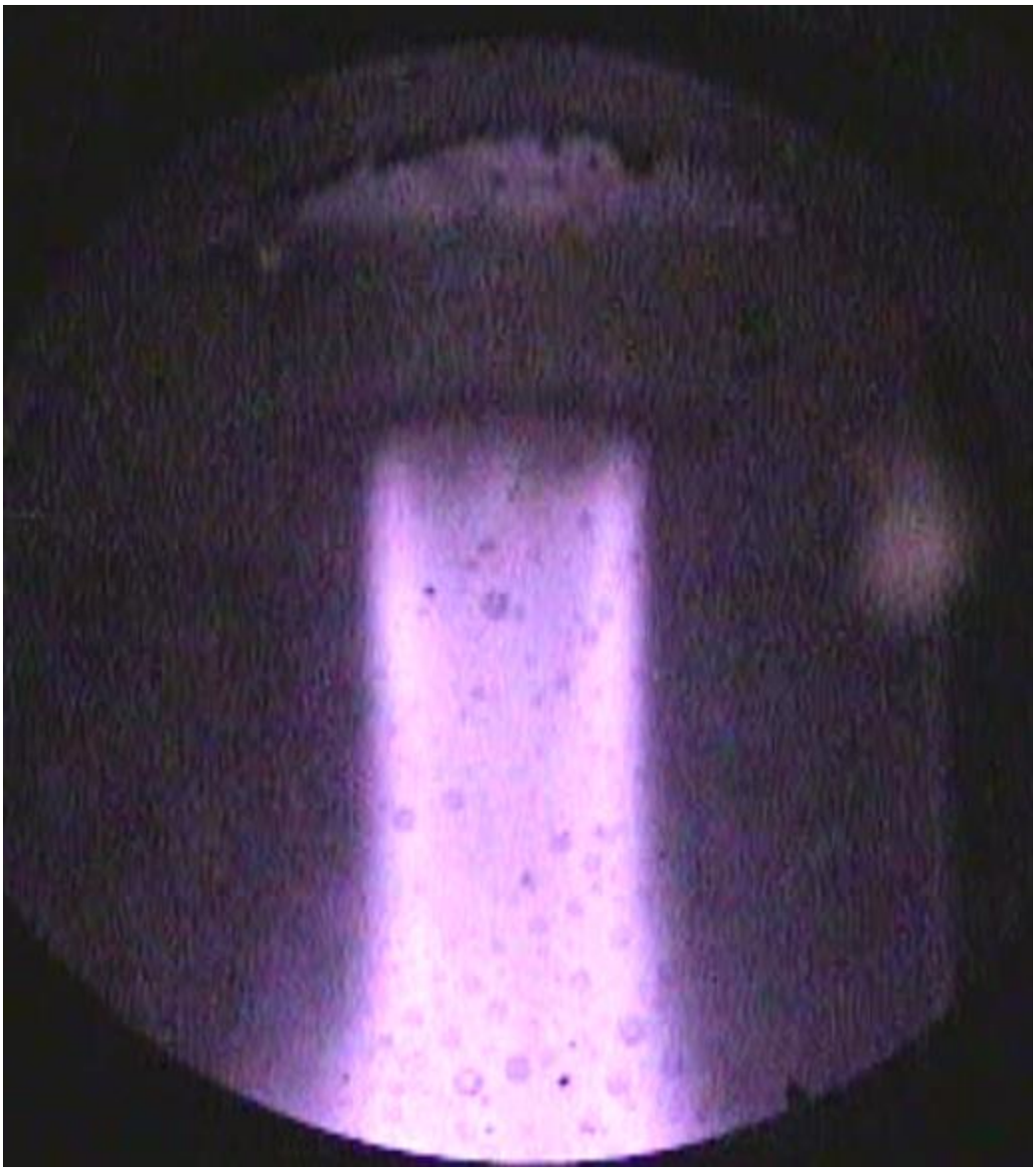

Figure 9: 50% H2-50% CO stabilized jet flame

Figure 10: 50% H2-50% CO jet flame retracting (i.e. flashback)

Flashback is induced by first setting the inlet air temperature, vessel pressure, and bulk velocity. Once conditions are set the operator introduces the fuel slowly into the premixer. A pilot flame is used to stabilize the main flame. When the stable flame is reached the operator then slowly increases the fuel flow (i.e. equivalence ratio) until flashback is observed. When flashback is observed the operator immediately shuts the fuel mitigating the flame. Flashback is

noted most dominantly by a spike in differential pressure between the premixer and combustor as seen in Figure 11.

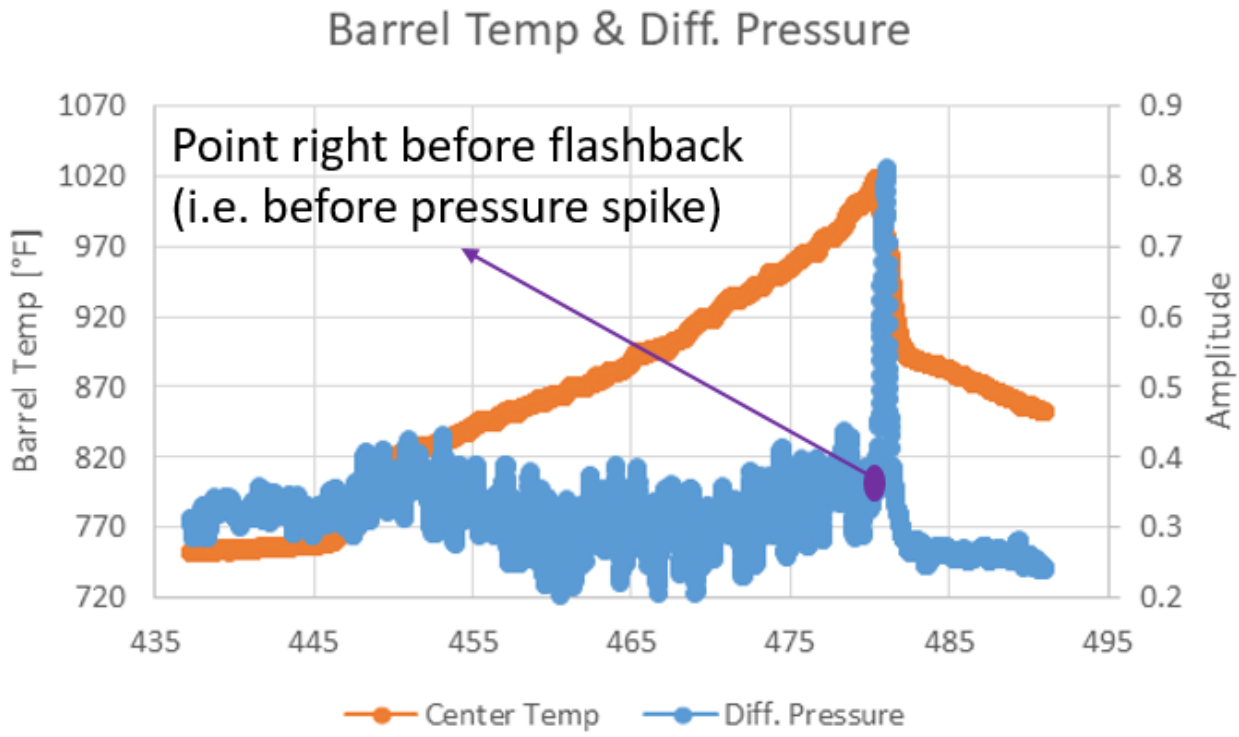

Figure 11: Pressure/Amplitude spike between the premixer and combustion zone

A total of 40 test cases were conducted and analyzed in this paper.

4.2 Turbulence Intensity Premixer Design

The premixer design for the jet flame study can be seen in Figure 12. The preheated air enters the Venturi and pure hydrogen, as the fuel, is injected through the low-pressure section, thus leading to an adequate mixing level. The fuel-air mixture is then channeled through a perforated plate (Figure 13) that is located after the exit of the venture, thus creating a uniform velocity profile, and it acts as a flame arrestor when flashback occurs. After the fuel-air mixture

passes the perforated plate it feeds through a premixing pipe with an inner diameter of 35 mm and length of 30 cm. The premixing tube is long enough to achieve a uniform concentration and fully develop the flow by the time it travels the pipe length and encounters a turbulence intensity generator plate. The flame is contained inside a quartz tube combustor liner that has a 15 cm inner diameter and is 19 cm in length. Two thermocouples were cemented to opposite sides of the burner tip to measure the tip temperature continuously. A pressure transducer was used to record the pressure drop across the premixer and combustion chamber (unconfined flame), which spiked when flashback occurs. The flame propagates upstream of the flow at the onset of flashback, which causes a significant elevation in the tip temperature and pressure difference.

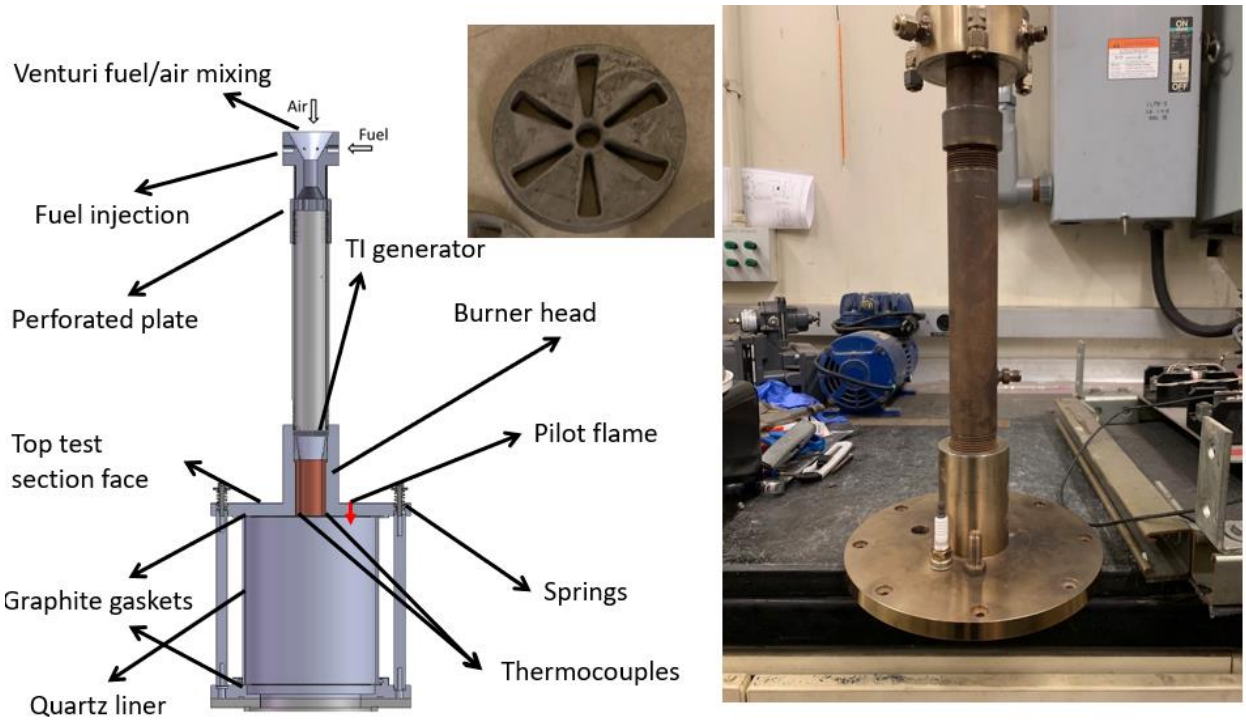

Figure 12: Premixer Setup

Figure 13: Perforated Plate

4.3 Turbulence Intensity Generator and LDV

Past experimental studies of premixed flames in intense isotropic turbulence was investigated by Bédat et al. [98], which shows minimal changes in flame structure. A series of perforated plates were created, a method from [99], to incorporate into an original premixed fully developed test rig with an exit diameter of 2.54 cm. The blockage ratio concept was designed using the help of data published by Marshall et al. [100] that allow for similar radial and tangential velocities. The specific turbulence intensity generator has an 81% backflow ratio, is 3.81 cm in diameter and 0.64 cm in thickness (Figure 14) and is placed 8.63 cm from the exit of the burner.

Figure 14: 81% blockage ratio turbulence intensity generator

Laser Doppler Velocimetry (LDV) was used to measure the velocity profile and turbulence intensity near the burner exit plane (7 mm above exit). In the LDV setup, air and water mix up-stream of the burner exit, which allows the LDV to track the water particles. The air flow was captured using a ¼" sonic orifice plate made in-house. The velocity was set to 35 m/s for consistancy. The setup of the premixer and LDV can be seen in Figure 15. The LDV utilizes a 4 watt Coherent Innova 90C-A4 argon-ion laser coupled with a TSI LDV system. The laser beam is separated by an Aerometrics Fiberlight multi-color beam separator for measuring three velocity components. For this experiment, only axial and radial velocity components are measured as the work from [100] indicaates that with the plate design the radial and tangnetial velocity profile are identical. Transmitting and receiving optics are done by a LDV00302 backscatter transceiver, consisting of a 261 mm focal length, a PDM 1000 photodetector, and a FSA 4000 signal processor unit. Technical stats for the transmitter optics for Channel 1 (axial

beams): wavelength of 514.5 nm, focal length of 500 nm, beam separation of 20 nm, laser beam diameter of 1.77 mm, beam expander ratio of 2, expanded beam separation of 40 nm, expanded beam diameter of 3.54 nm, fringe spacing of 6.4364 μm, beam waist of 92.53 μm, and a bragg cell frequency of 40 MHz. Channel 2 of the laser (radial) mainain the same optics characteristic as Channel 1 except for the following: wavelength of 488 nm, fringe spacing 6.1049 μm, and a beam waist of 87.76 μm.

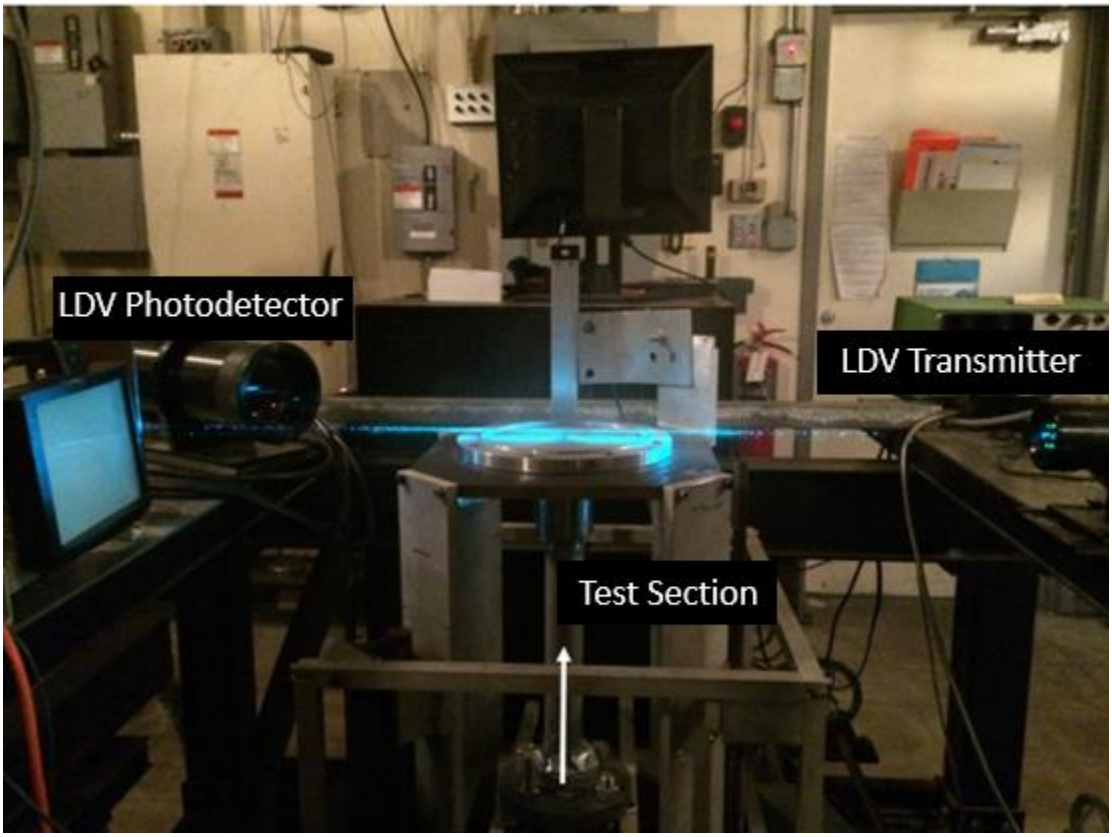

Figure 15: LDV Setup

The results and discussion will go through the phase of first discussing the design of experiment used with the LDV to receive consistent and realistic turbulence intensity values based off of typical jet flame flow between 4-6% as investigated by [105]. Next the results of the

turbulence intensity generator will be discussed and how it was utilized in the premixer design. The CFD gradient values are then investigated and analyzed for the 2 cases of flashback testing (5.4 and 15.7% turbulence intensity cases). Lastly, the discussion of the effect of turbulence intensity on boundary layer flashback will be explained.

5.0 Results and Discussion

5.1 LDV Study on the Effects of Factors on Turbulence Intensity

LDV was utilized as the instrumentation to evaluate turbulence intensity. To assure consistent results a 2 level factorial, with 2 center points, design of experiment was conducted to observe if the Laser Doppler Velocimetry main settings had a significant impact on measured turbulence intensity. The span of a base test to evaluate the effects of PMT Voltage, Burst Threshold, and laser power on the value of turbulence intensity was conducted and can be seen in Figure 16. The design of experiment is meant to evaluate the 4 factors mentioned above and develop a correlation between those values and turbulence intensity.

Factors	PMT Voltage	Burst Threshold	Laser Power	Turbulence Intensity
	[V]	[mV]	[W]	[%]
LOW	400	35	1.5	X
MIDDLE	500	42.5	1.75	X
HIGH	600	50	2	X
Test 1	600	50	2	13.1
Test 2	600	50	1.5	13.9
Test 3	600	35	2	12.6
Test 4	600	35	1.5	12.9
Test 5	400	50	2	17.9
Test 6	400	50	1.5	17.8
Test 7	400	35	2	17.3
Test 8	400	35	1.5	17.1
Test 9	500	42.5	1.75	15.4
Test 10	500	42.5	1.75	15.5

Figure 16*:* DOEx test matrix

Certain factors are shown to affect the turbulence intensity value. These results were inputted in the Design Expert® software to observe the sensitivity of each factor on the response (turbulence intensity). The Half-Normal plot seen below in Figure 17 shows that PMT Voltage significantly impacts the turbulence intensity measurements of the LDV.

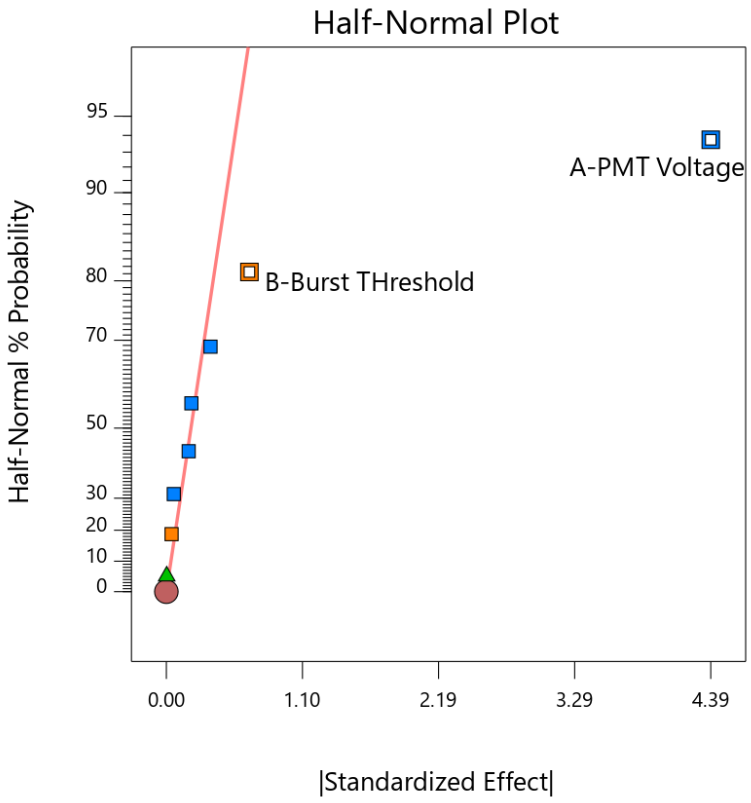

Figure 17: Half-Normal Plot

To visualize the results in a common fashion using Design Expert® a “cube” was produced showing the change of turbulence intensity on the other factors (Figure 18).

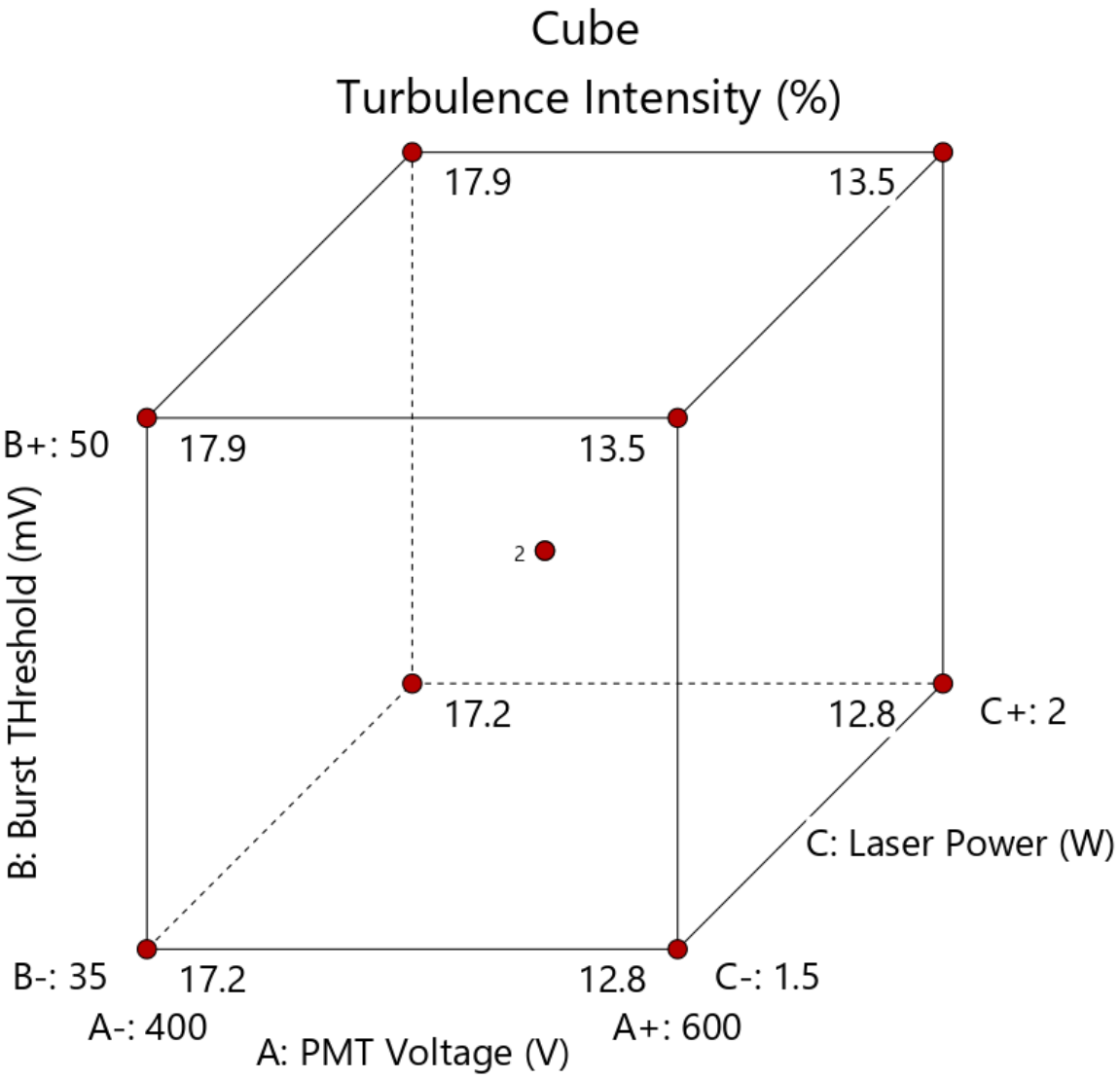

Figure 18: Cube Turbulence Intensity

The above figure indicates that the larger the PMT Voltage is, the lower the turbulence intensity value becomes. The fit statistics show a linear regression of 98.96 % and the other details are shown in Figure 19.

Std. Dev.	0.2628		**R^2**	0.9896
Mean	15.35		**Adjusted R^2**	0.9861
C.V. %	1.71		**Predicted R^2**	0.9732
			Adeq Precision	30.4160

Figure 19: Fit statistics

The finalized data (not shown) indicated no significant difference between 600 V and 700 V. 700 V was chosen as the PMT Voltage to assure a plateau of turbulence intensity was reached. The higher PMT voltage also represented values of turbulence intensity that were similar to literature as indicated in [97]. This study concludes that a fully developed and steady jet flame produces a turbulence intensity value between 4 to 6%. The final data for the fully developed jet flame in this work was 5.4%. The final equation in terms of actual factors is displayed in Figure 20, which was used to calculate the turbulence intensity value from the LDV.

Turbulence Intensity	=
+24.44560	
-0.021931	* PMT Voltage
+0.044644	* Burst THreshold

Figure 20: Turbulence intensity equation in terms of laser settings

The LDV settings were finalized and operated on the following settings:

- PMT Voltage: 700V
- Burst Threshold: 35 mV
- Laser Power: 2.0W (25 mW/each beam)

5.2 LDV Results for 81% Blockage Ratio

Multiple turbulence intensity plates were made and tested (Figure 21). The 81% Blockage ratio plate was chosen as the main design as mentioned in the "Methods" section. This plate allowed the turbulence intensity to increase from the stock 5.4% to 15.7%, roughly 3 times the original value. The turbulence intensity was measured using Laser Doppler Velocimetry (LDV). The results were then compared to those produced by Marshall et al. [100] who did a similar study. The two data sets show similarities and can be overlapped to show similar results of turbulence intensity for a given backflow ratio as seen in Figure 22. Based on the comparison and fact that Marshall's work verified performance at elevated pressure and temperature, it can be said that the produced turbulence intensity stays true at the gas turbine conditions tested in this work. The turbulence intensity is purely a function of the blockage ratio at a fixed distance from the exit.

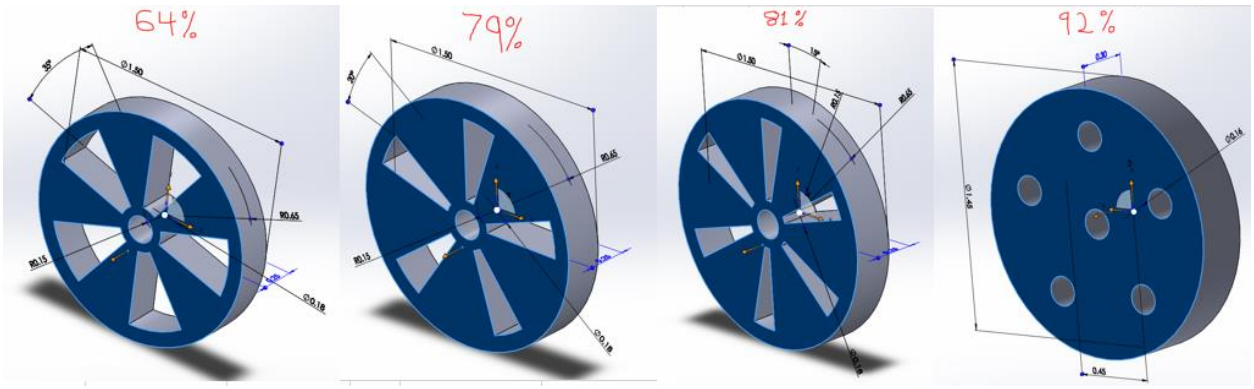

Figure 21: Turbulence intensity generator designs

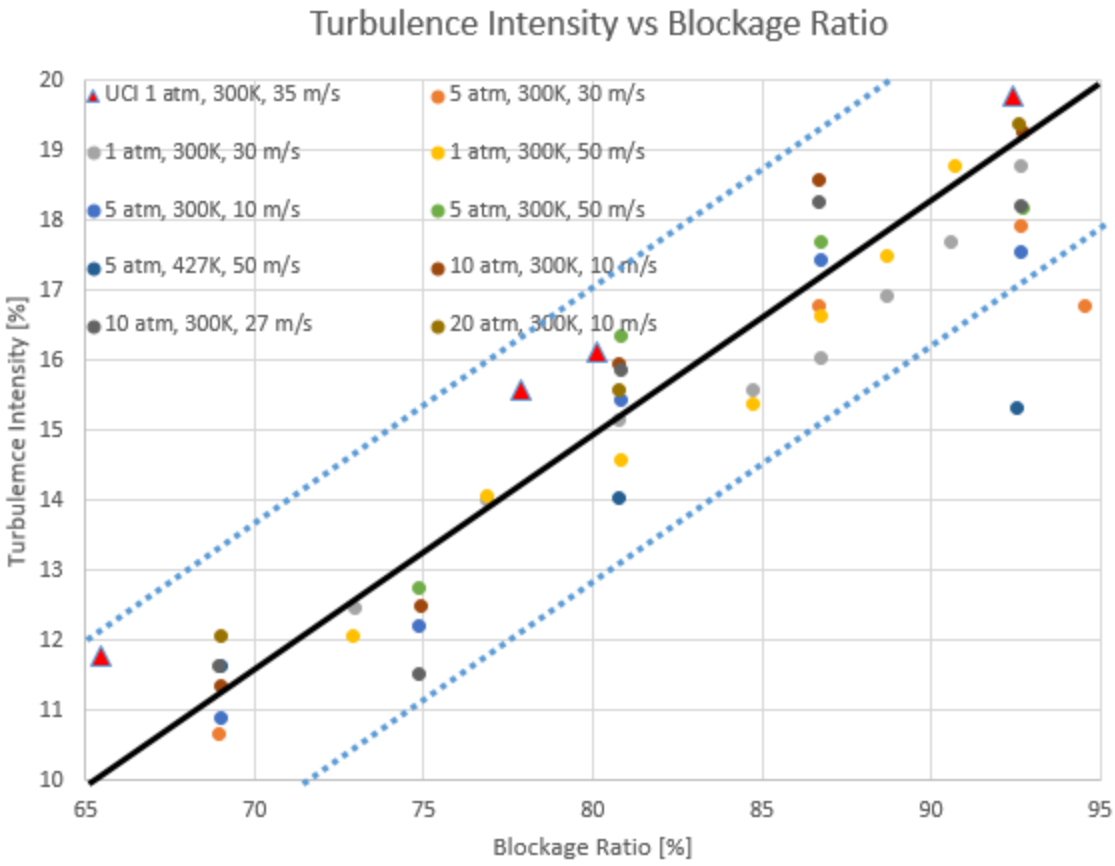

Figure 22: Experimental data of turbulence intensity vs blockage ratio using LDV against Marshall et al. [100]

5.3 CFD Study of Velocity Gradient

Since a perturbation in the flow for the modified premixer design was introduced by the turbulence generator, the flow will not be fully developed. As a result, a Blasius equation for velocity gradient "technically" cannot be utilized. To capture the velocity gradient of the non-uniform flow ANSYS® Fluent was utilized for CFD analysis. The following criteria were used to find the velocity gradient via CFD for the correlation using a k-epsilon with enhanced wall treatment:

- Meet Fluent stated mesh quality standards
    - ✓ Skewness < 0.9
    - ✓ Orthogonal Quality > 0.05
- Resolve y+ values to be less than or equal to 1
    - ✓ States boundary layer is resolved (needed for turbulence model)
- Extract velocity gradient value at the quench distance (Figure 4) via the equation below [61], where the predicted g_c is obtained from Eq. 5.2 and S_L obtained via Chemkin®.

$$\delta_q = 7.3 * \frac{S_L}{g_c}$$

The results for a certain case are shown in this paper. The velocity profile for both turbulence intensity cases are plotted below in Figure 23. The velocity profile is shown from the core of the flow out to one wall, with the other excluded because it is symmetric. The difference in velocity profile is due to the perturbation introduced in the flow. Also, keep in mind that conditions are not the same between experimental runs as it is difficult to maintain exact conditions, so small discrepancy between the cases are evident, but do not impact results.

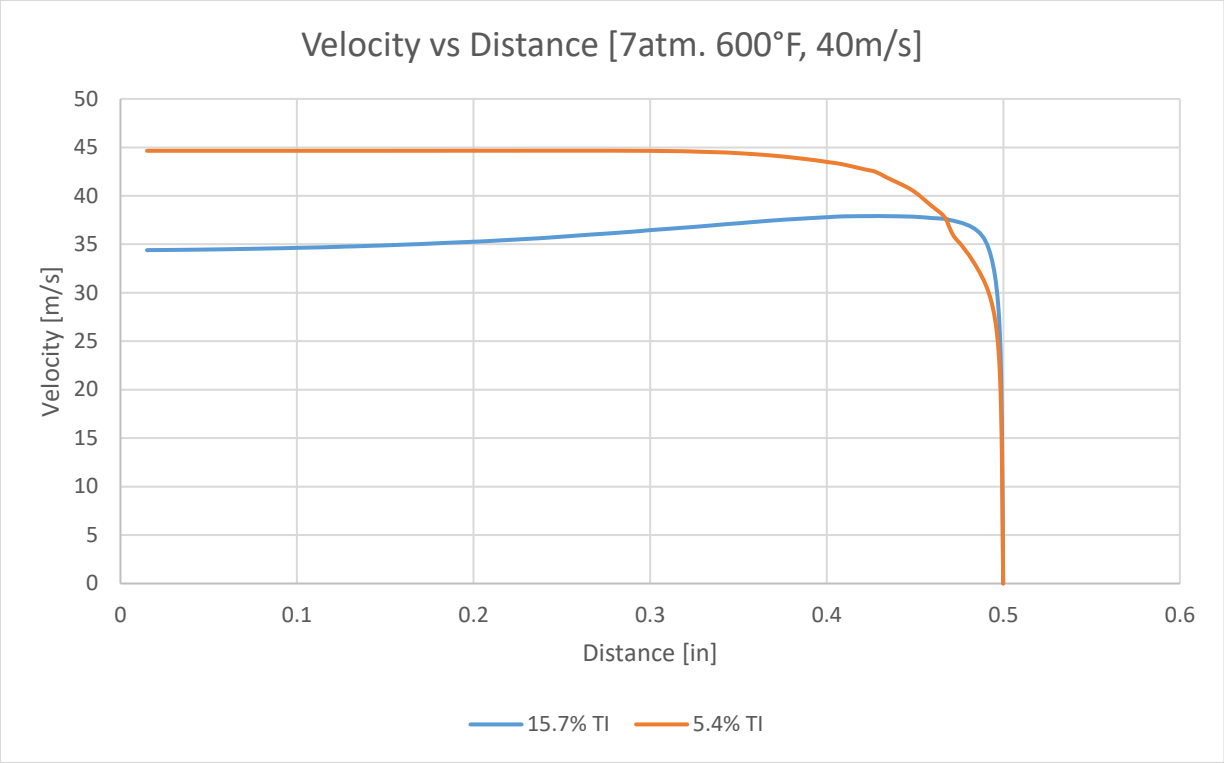

Figure 23: Velocity CFD

The velocity profile for the 15.7% turbulence intensity case is plotted in Figure 24. The velocity profile comes from one plane through the center of the premixer exit. If the cut was taken 90° from this image the velocity profile would shift across the y-axis (i.e. same profile but the peak velocity would occur on the opposite side.)

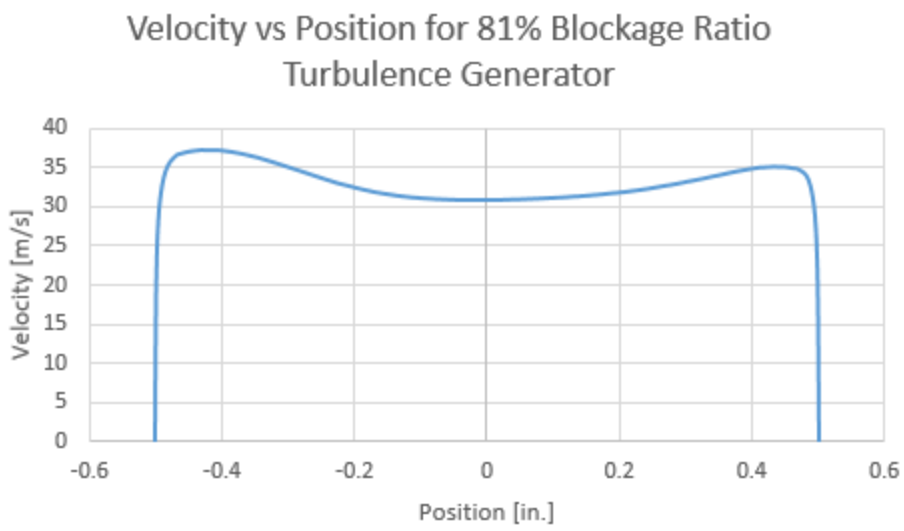

Figure 24: Velocity Profile for 81% blockage ratio turbulence generator

The velocity gradient is plotted, and the value is extracted at the quench distance of each case. The 5.4% turbulence intensity basically being the Blasius solution compares very similarly to the non-fully developed flow for all data runs captured. Results remained consistent between the different turbulence intensity values at given conditions. The CFD results indicate that the turbulence intensity is dampened at the wall, resulting in comparable gradient values (Figure 25) Hence, CFD may not be needed to capture velocity gradient for non-fully developed flow for boundary layer flashback.

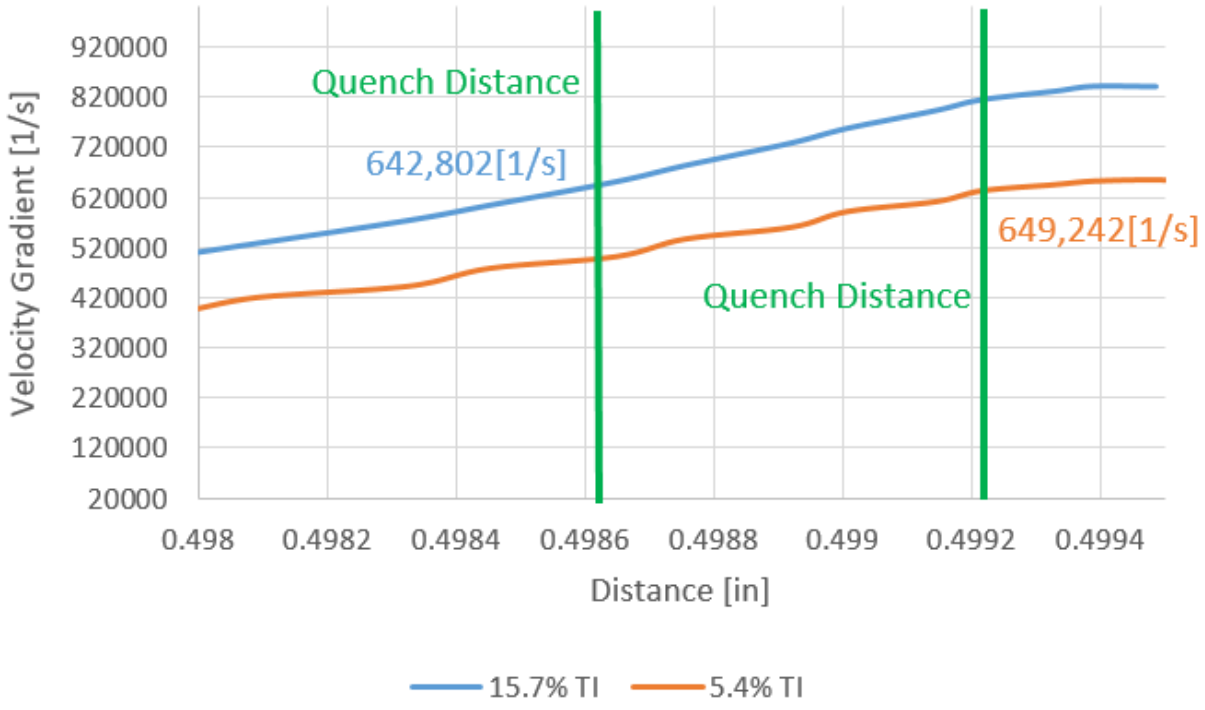

Figure 25: Velocity gradient at quench distance via CFD

The quench distance is a function of laminar flame speed and actual critical velocity gradient, hence the quench distance will vary slightly due to small discrepancies in bulk flow velocity, inlet temperature, operating pressure, and equivalence ratio at flashback. Typical quench distance for stoichiometric hydrogen flames at atmospheric conditions is 0.025" (0.64 mm) as mentioned in "An Introduction to Combustion Concepts and Applications: by Stephen R. Turns. The quench distance for the experiments mentioned in this paper are smaller because of decreased laminar flame speed at high operating temperature and pressure. To re-iterate, the diameter of the premixer in the experiment is 1" and the quench distance in Figure 25 is the distance from the wall placing the origin at the center of the flow.

5.4 High Pressure and Temperature Study of the Effects of Turbulence Intensity on Boundary Layer Flashback

When performing flashback testing at high pressure and temperature a few measures are taken to assure consistent data. Pre-heat temperature, pressure, and bulk velocity are held constant while the fuel is slowly increased until flashback occurs. Once, flashback is reached the fuel is immediately shut-off to arrest the flame from melting components of the premixer. Test were conducted from a range of 3-7 atm., 400-600°F, and a bulk velocity of 25-40m/s in order to span the Damköhler number and rig capabilities. The Damköhler number is defined as the flow time scale to the combustion time scale and the developed correlation takes into account the effect of equivalence ratio [3,67].

$$Da = Const.\, Le^{1.68}.\, Pe_f{}^{1.91}.\left(\frac{T_u}{T_0}\right)^{2.57}.\left(\frac{T_{tip}}{T_o}\right)^{-0.49}.\left(\frac{P_u}{P_0}\right)^{-2.1} \qquad Eq.\,5.1$$

The actual Damköhler number is represented as seen in Eq. 5.2 below, where S_L is the laminar flame speed, α is the thermal diffusivity, an g_c is the critical velocity gradient.

$$Da = \frac{{S_L}^2}{\alpha \cdot g_c}, \qquad Eq.\,5.2$$

The flashback model developed at PSI (Paul Sherrer Institute) shows the dependence on the ratio of the turbulent flame speed (global consumption speed method) to the laminar flame speed, which is represented as a function of turbulence intensity (u') as seen in Eq. 5.3 [95] though it does not capture the thermal coupling effects that Eq. 5.1 does [96].

$$Da = Const.\,Le.\,Pe_f^{0.37}\left(\frac{u'}{S_L}\right)^{-0.63}\left(\frac{T_u}{T_0}\right)^{0.63}\left(\frac{P_u}{P_0}\right)^{-0.63} \qquad Eq.\,5.3$$

If the velocity gradient drops below the critical velocity gradient, flashback is induced [96]. Flashback is a highly coupled problem and because the turbulence intensity is varied the velocity gradient at the wall can be affected in turn. ANSYS® Fluent is used to determine the velocity gradient at the wall for each flashback condition.

The leading coefficient in the Damköhler expression is shifted via the value of the velocity gradient. This leading coefficient can capture synthetic shifts in critical velocity gradient for the prediction model. Therefore, even if CFD is not resolving the boundary layer as long as the approach is consistent it may not matter. This does imply that the leading term plays a strong role in the predictive ability, thus a consistent CFD method must be used to establish a predictive ability. The approach method is discussed in section 5.3, which is used to ensure consistent results. The method in 5.3 compared within 1% of the gradient from the Blasius profile showing that CFD is resolving the boundary layer properly via this method.

A course mesh was compared to the resolved boundary layer mesh method (y+ less than or equal to 1) and results plotted in Figure 26.

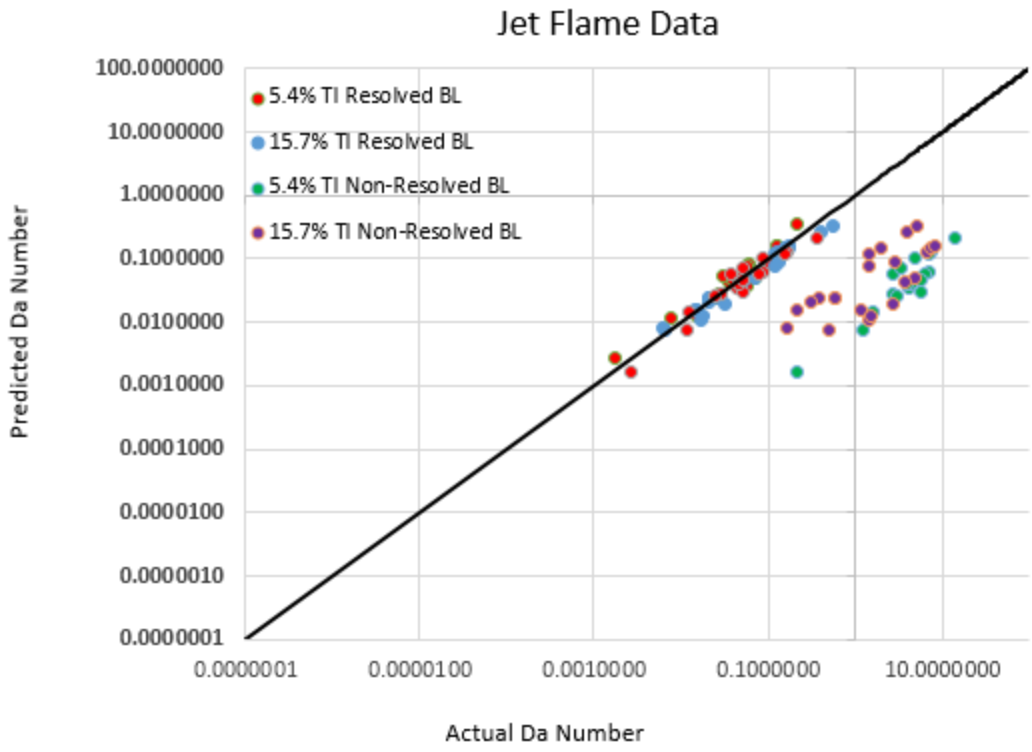

Figure 26: Velocity gradient difference creates a synthetic shift in data

The results plotted above in terms of turbulence intensity will be discussed below shortly. The velocity gradient extracted from CFD for the resolved boundary layer were values in the 100,000's while the unresolved boundary layer resulted in values around the 1,000's. The constant in the Damköhler equation (Eq. 5.3) shifted from 2.5*10^-5 for the resolved boundary layer to 9*10^-4 for the unresolved boundary layer (i.e. course mesh) for the data to fall on the line and allow the model the capability to predict flashback conditions.

Previous testing by Kalantari et al. [96] used eq. 2.6-2.8, Blasius profile, to determine the velocity gradient at the wall since the flow was fully developed. The corresponding results for multiple fuels, burner heads, preheat temperatures, and pressures are seen in Figure 27. It is

important to note that all the tests seen below were conducted with a constant turbulence intensity, thus the effect was not studied until now.

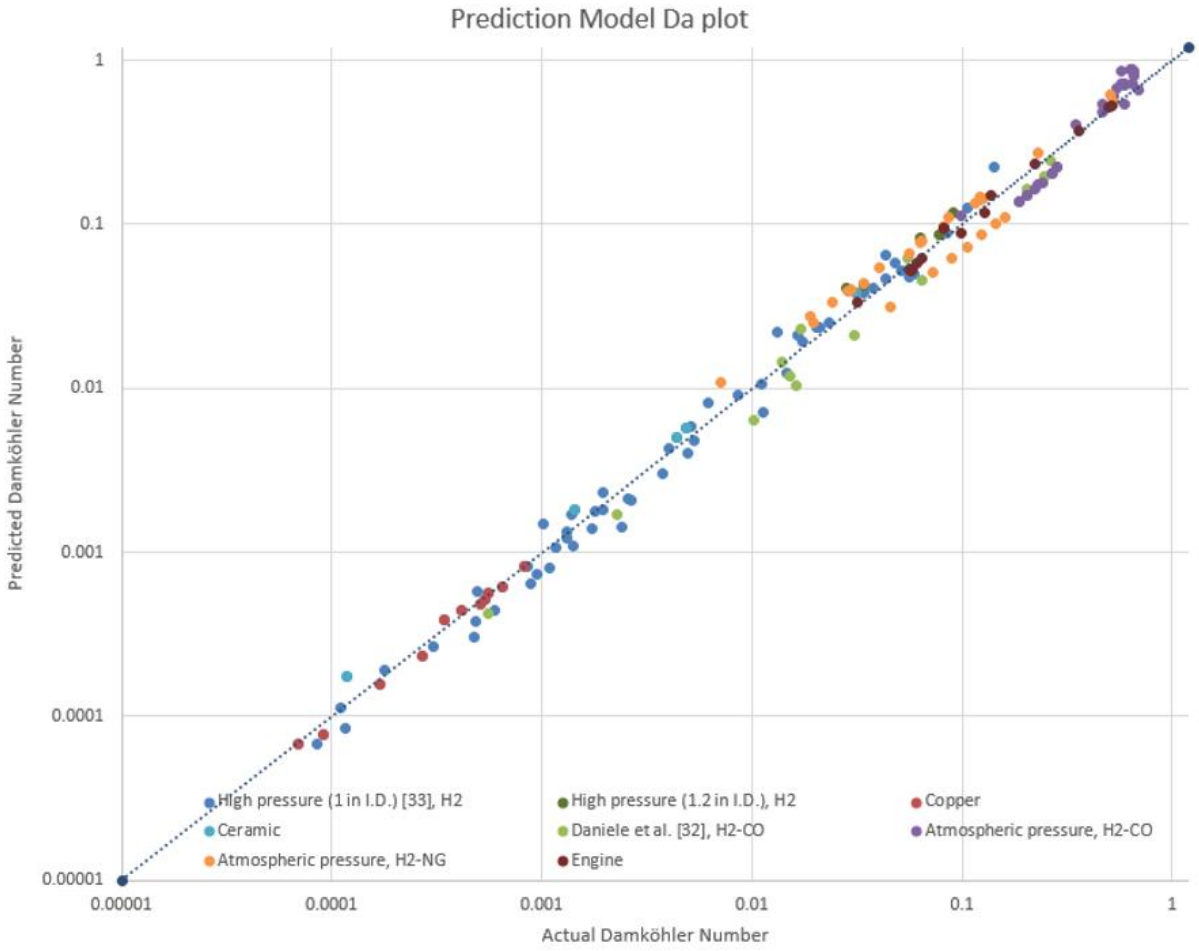

$$Da = 5.8 * 10^{-6} * Le^{1.68}.Pe_f{}^{1.91}.\left(\frac{T_u}{T_0}\right)^{2.57}.\left(\frac{T_{tip}}{T_o}\right)^{-0.49}.\left(\frac{P_u}{P_0}\right)^{-2.1}$$

Figure 27: Da plot of multiple setups and parameters with no turbulence intensity factor

When post-processing the data between the 5.4% and 15.7% turbulence intensity setup, it was observed that the burner tip temperature at flashback for the non-modified setup was 2.8% less than the modified case. The equivalence ratio at flashback between the two cases show that

the higher turbulence intensity flame had lower flashback propensity at 3 and 7 atm. but higher flashback propensity at 5 atm., though these values were within 2% of each other.

At 3 atm. the 15.7% turbulence intensity flame had a higher tip temperature but was able to reach higher equivalence ratios at flashback by an average of 6.1 and 9.2%, respectively. At 5 atm. the 15.7% turbulence intensity plate had a higher tip temperature but a lower equivalence ratio up to flashback by an average of 2.7 and 6.0%, respectively. At 7 atm. the 15.7% turbulence intensity plate had a lower tip temperature but could go to higher equivalence ratios up to flashback by an average 0.5 and 3.1%, respectively. From these data sets we cannot conclude that the higher turbulence intensity plate has a differing effect on flashback propensity due to the combined uncertainty of the instrumentation. Results of low vs high turbulence intensity value at the exit of the premixer shows no effect on BLF within a 2% uncertainty. The combined recorded equivalence ratio and tip temperature were all within 2% of each other. The data are plotted on the prediction model formula in Figure 28.

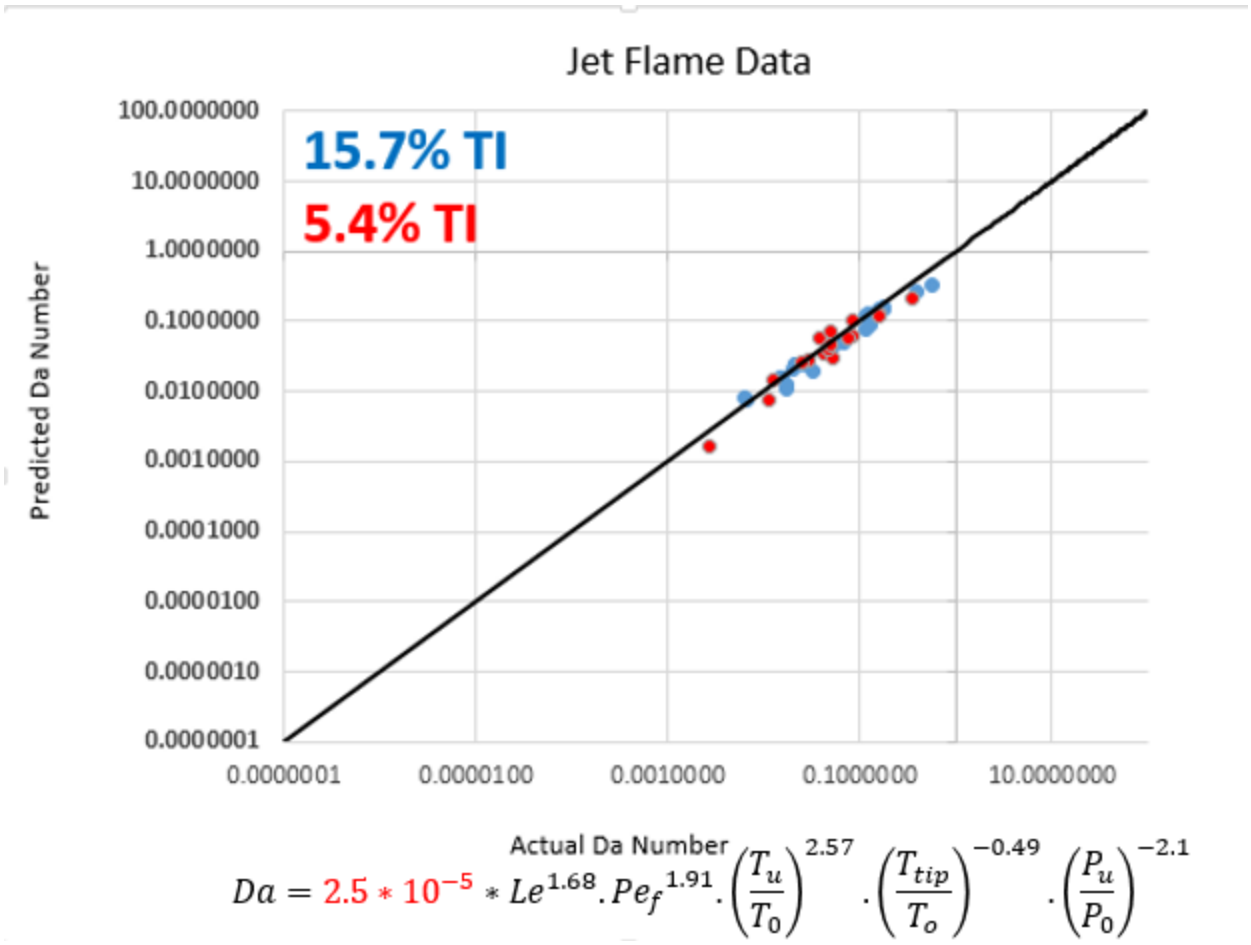

Figure 28: Da plot for turbulence intensity data

Theoretically, the flame speed increases with turbulence intensity but a general increase in flashback propensity is not observed. This can potentially be attributed to the different velocity gradients near the wall or a buffered effect on turbulence intensity near the wall. If the actual velocity gradient drops below the critical velocity gradient, then flashback will occur. Overall it seems that bulk flow turbulence intensity may not have a profound effect on boundary layer.

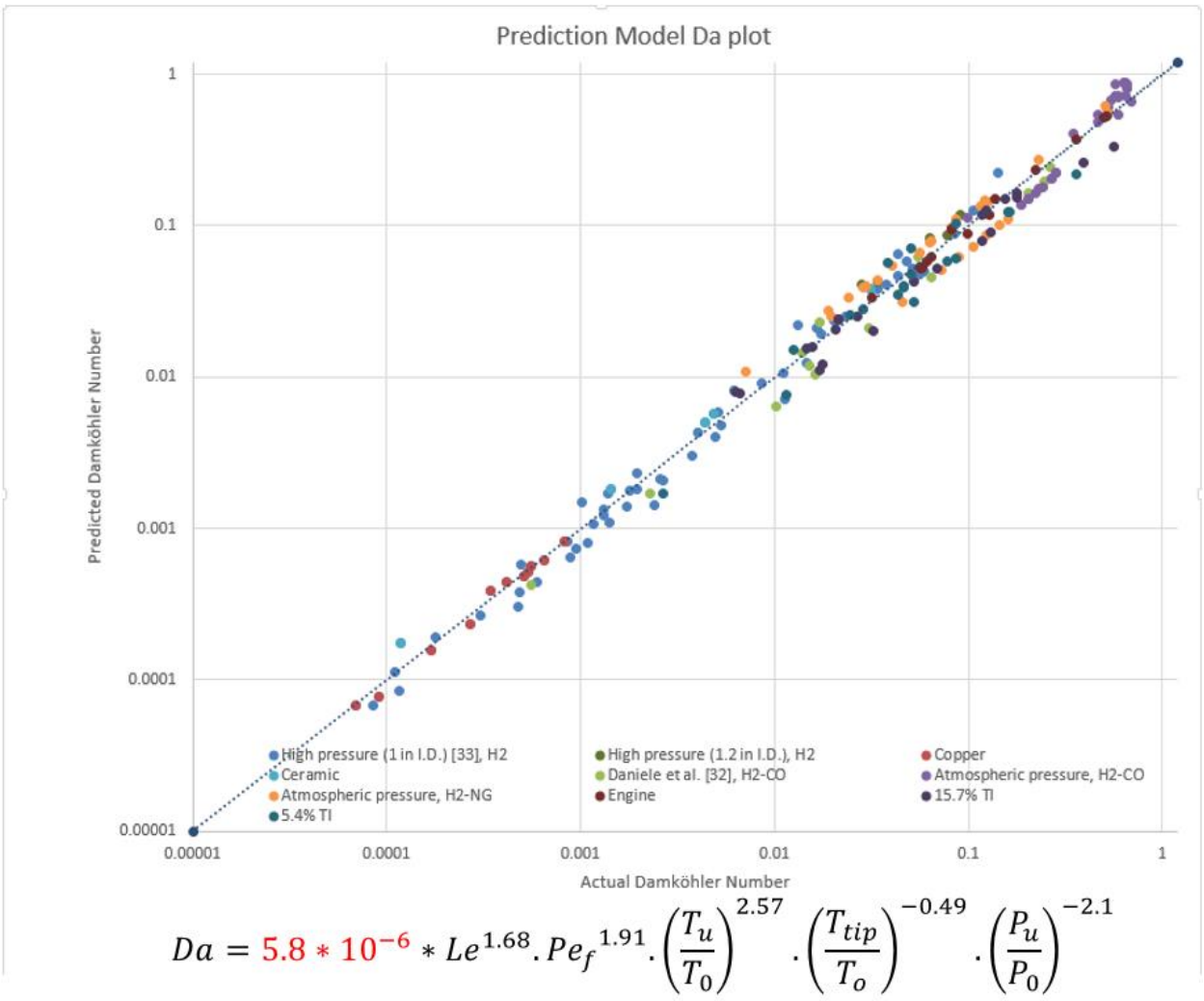

$$Da = 5.8 * 10^{-6} * Le^{1.68} . {Pe_f}^{1.91} . \left(\frac{T_u}{T_0}\right)^{2.57} . \left(\frac{T_{tip}}{T_o}\right)^{-0.49} . \left(\frac{P_u}{P_0}\right)^{-2.1}$$

Figure 29: Da plot of multiple setups and parameters

6. Summary, Conclusions, and Recommendations

6.1 Summary

The effect of turbulence intensity on boundary layer flashback propensity was studied. A range of temperatures (400-600°F) and pressures (3-7 atm.) were utilized to study the effect with the use of 100% hydrogen as the fuel. A perforated plate with an 81% backflow ratio was designed and developed with information from Marshall et al. [100], and LDV was used to obtain the turbulence intensity value the plate produced at the core. The 81% backflow plate was capable of nearly tripling the turbulence intensity of the original, non-modified, premixer. Experimental test were performed to compare both cases for BLF propensity. Experimental test between both cases showed no difference in flashback propensity (i.e. equivalence ratio and barrel temperature).

ANSYS® Fluent was used to obtain the velocity gradient since the Blasius equation could not be utilized. The introduction of a turbulence intensity generator near the exit of the premixer created the non-fully developed flow. A series of requirements for meshing the cold flow was developed and utilized to obtain the velocity gradient at the quench distance, equivalent to penetration distance, though no specific equation for quench distance has been utilized for multiple operating conditions. CFD results concluded that the velocity gradient for both the fully and non-fully developed flow were nearly equivalent for the same operating conditions. From this, it was concluded that the turbulence intensity was dampened at the wall, thus not playing a strong role in boundary layer flashback. This result stated that modeling the premixer in CFD is not required and instead the Blasius gradient can be utilized as a replacement.

The similarity of the test rig utilized in this work and by that by Kalantari [67], for flashback prediction modeling, show that the data taken from the test rig in this work fall on top to that of Kalantari' verifying that the model prediction can be utilized for different setup conditions.

6.2 Conclusions

- **Equivalence ratio and tip temperature had no notable change at flashback with a change in turbulence intensity (within 2%)**

  The equivalence ratio and tip temperature for the low and high turbulence intensity flow remained equivalent during experimental testing. This was the initial step to conclude turbulence intensity does not play a role in BLF. The high turbulence intensity value allows the premixer to better mix the fuel and air mixture, thus reducing overall emissions. It was later concluded that the turbulence intensity at the wall is dampened out.

- **Effect of turbulence intensity on boundary layer flashback**

  While an increase in turbulence intensity may help improve mixing, it may also lead to impacts on the overall operability of these systems including behavior such as flashback. Higher turbulence intensity is known to increase turbulent burning velocity, hence the question as to whether flashback propensity is affected is raised. Studies were conducted at pressures from 3 to 8 atm. with preheated reactants up to 750 deg. K. and pure hydrogen as the fuel was evaluated. The results show that even with significantly different turbulence intensities (ratio of flow centerline turbulence to centerline axial velocity) boundary layer flashback is not strongly affected. This is attributed to the role

of the quenching distance in connection with the boundary layer. Core flow flashback or other flashback mechanisms may be affected differently.

6.3 Recommendations

As the move towards hydrogen usage in gas turbines progress, a continued study of boundary layer flashback is necessary to assure safety in the operation. To properly/accurately capture the velocity gradient of the flow field a stronger developed equation for the penetration distance is needed. The equation should be in terms of operating conditions that affect the flow field such as temperature of the rim at flashback, operating pressure, and equivalence ratio and or Lewis number to capture the fuel characteristics. Also, a similar study of turbulence intensity effects on flashback propensity can be addressed further by moving the turbulence intensity generator closer to the exit of the burner rim to see if there reaches a point where the core turbulence intensity affects the turbulence intensity near the wall.

7. REFERENCES

1. Richards G., McMillian M., Gemmen R., Rogers W., Cully S. Issues for low-emission, fuel-flexible power systems. Prog Energy Combust Sci 2001;27:141–69. doi:10.1016/S0360-1285(00)00019-8.

2. McDonelll, V.G. and Klein, M. (2013). Ground Based Gas Turbine Combustion: Metrics, Constraints, And System Interactions, in *Gas Turbine Emissions*, T. Lieuwen and V. Yang (eds).

3. Lieuwen, T., McDonell, V., Santavicca, D., and Sattelmayer, T. (2008). Burner Development and Operability Issues Associated with Steady Flowing Syngas Fired Combustors (2008). *Combustion Science and Technology* vol. 180, pp. 1169-1192

4. Lefebvre A, Ballal D. Gas turbine combustion 2010.

5. Lieuwen T, McDonell V, Petersen E, Santavicca D. Fuel flexibility influences on premixed combustor blowout, flashback, autoignition, and stability. J Eng Gas Turbines Power 2008;130:011506. doi:10.1115/1.2771243.

6. Bickerstaff K, Walker G. Public understandings of air pollution: the 'localisation' of environmental risk. Glob Environ Chang 2001;11:133–45. doi:10.1016/S0959-3780(00)00063-7.

7. Bickerstaff K. Risk perception research: socio-cultural perspectives on the public experience of air pollution. Environ Int 2004;30:827–40. doi:10.1016/j.envint.2003.12.001.

8. Lieuwen T, McDonell V, Santavicca D, Sattelmayer T. Burner development and operability issues associated with steady flowing syngas fired combustors. Combust Sci Technol 2008;180:1169–92. doi:10.1080/00102200801963375.

9. Lieuwen T., Vigor Y. Combustion instabilities in gas turbine engines: Operational experience, fundamental mechanisms, and modeling. Prog Astronaut Aeronaut 2005. doi:10.2514/4.866807.

10. Howarth RW, Ingraffea A, Engelder T. Natural gas: Should fracking stop? Nature 2011;477:271–5. doi:10.1038/477271a.

11. Wang Q, Chen X, Jha AN, Rogers H. Natural gas from shale formation – The evolution, evidences and challenges of shale gas revolution in United States. Renew Sustain Energy Rev 2014;30:1–28. doi:10.1016/j.rser.2013.08.065.

12. Demirbas A. Progress and recent trends in biofuels. Prog Energy Combust Sci 2007;33:1–18. doi:10.1016/j.pecs.2006.06.001.

13. Rostrup-Nielsen JR, Sehested J, Nørskov JK. Hydrogen and synthesis gas by steam- and C02 reforming. Adv Catal 2002;47:65–139. doi:10.1016/S0360-0564(02)47006-X.

14. Xu J, Froment GF. Methane steam reforming, methanation and water-gas shift: I. Intrinsic kinetics. AIChE J 1989;35:88–96. doi:10.1002/aic.690350109.

15. Bolland O, Undrum H. A novel methodology for comparing CO2 capture options for natural gasfired combined cycle plants. Adv Environ Res 2003;7:901–11. doi:10.1016/S1093-0191(02)00085

16. Descamps C, Bouallou C, Kanniche M. Efficiency of an integrated gasification combined cycle (IGCC) power plant including CO2 removal. Energy 2008;33:874–81. doi:10.1016/j.energy.2007.07.013.

17. Minchener AJ. Coal gasification for advanced power generation. Fuel 2005;84:2222–35. doi:10.1016/j.fuel.2005.08.035.

18. Haszeldine RS. Carbon Capture and Storage: How Green Can Black Be? Science (80-) 2009;325:1647–52. doi:10.1126/science.1172246.

19. Herzog HJ. What Future for Carbon Capture and Sequestration? Environ Sci Technol 2001;35:148A–153A. doi:10.1021/es012307j.

20. Turner JA. Sustainable Hydrogen Production. Science (80-) 2004;305:972–4. doi:10.1126/science.1103197.

21. Chiesa P, Lozza G, Mazzocchi L. Using Hydrogen as Gas Turbine Fuel. ASME Turbo Expo, 2003, p. 163–71. doi:10.1115/GT2003-38205.

22. Plee SL, Mellor AM. Review of flashback reported in prevaporizing/premixing combustors. Combust Flame 1978;32:193–203. doi:10.1016/0010-2180(78)90093-7.

23. Thibaut D, Candel S. Numerical study of unsteady turbulent premixed combustion: application to flashback simulation. Combust Flame 1998;113:53–65. doi:10.1016/S0010-2180(97)00196-X.

24. Driscoll JF. Turbulent premixed combustion: Flamelet structure and its effect on turbulent burning velocities. Prog Energy Combust Sci 2008;34:91–134. doi:10.1016/j.pecs.2007.04.002.

25. Lipatnikov AN, Chomiak J. Molecular transport effects on turbulent flame propagation and structure. Prog Energy Combust Sci 2005;31:1–73. doi:10.1016/j.pecs.2004.07.001.

26. Kido H, Nakahara M, Nakashima K, Hashimoto J. Influence of local flame displacement velocity on turbulent burning velocity. Proc Combust Inst 2002;29:1855–61. doi:10.1016/S15407489(02)80225-5.

27. Borghi R. Turbulent combustion modelling. Prog Energy Combust Sci 1988;14:245–92. doi:10.1016/0360-1285(88)90015-9.

28. Borghi R. On the structure and morphology of turbulent premixed flames. Recent Adv. Aerosp. Sci., Springer US; 1985, p. 117–38. doi:10.1007/978-1-4684-4298-4_7.

29. Kwon O., Faeth G. Flame/stretch interactions of premixed hydrogen-fueled flames: measurements and predictions. Combust Flame 2001;124:590–610. doi:10.1016/S0010-2180(00)00229-7.

30. Kobayashi H, Kawabata Y, Maruta K. Experimental study on general correlation of turbulent burning velocity at high pressure. Symp Combust 1998;27:941–8. doi:10.1016/S00820784(98)80492-X.

31. Kobayashi H, Tamura T, Maruta K, Niioka T, Williams FA. Burning velocity of turbulent premixed flames in a high-pressure environment. Symp Combust 1996;26:389–96. doi:10.1016/S00820784(96)80240-2.

32. Koroll GW, Kumar RK, Bowles EM. Burning velocities of hydrogen-air mixtures. Combust Flame 1993;94:330–40. doi:10.1016/0010-2180(93)90078-H.

33. Bradley D, Lawes M, Liu K, Mansour MS. Measurements and correlations of turbulent burning velocities over wide ranges of fuels and elevated pressures. Proc Combust Inst 2013;34:1519–26. doi:10.1016/j.proci.2012.06.060.

34. Benim A, Syed K. Flashback mechanisms in lean premixed gas turbine combustion. Academic Press; 2014.

35. Billant P, Chomaz J-M, Huerre P. Experimental study of vortex breakdown in swirling jets. J Fluid Mech 1998;376:S0022112098002870. doi:10.1017/S0022112098002870.

36. Leibovich S. The structure of vortex breakdown. Annu Rev Fluid Mech 1978;10:221–46. doi:10.1146/annurev.fl.10.010178.001253.

37. Konle M, Kiesewetter F, Sattelmayer T. Simultaneous high repetition rate PIV--LIF-measurements of CIVB driven flashback. Exp Fluids 2007;44:529–38. doi:10.1007/s00348-007-0411-2.

38. Asato K, Wada H, Hiruma T, Takeuchi Y. Characteristics of flame propagation in a vortex core: Validity of a model for flame propagation. Combust Flame 1997;110:418–28. doi:10.1016/S00102180(97)00082-5.

39. Duwig C, Fuchs L. Large eddy simulation of vortex breakdown/flame interaction. Phys Fluids 2007;19:075103. doi:10.1063/1.2749812.

40. Konle M, Sattelmayer T. Interaction of heat release and vortex breakdown during flame flashback driven by combustion induced vortex breakdown. Exp Fluids 2009;47:627–35. doi:10.1007/s00348-009-0679-5.

41. Ishizuka S. Flame propagation along a vortex axis. Prog Energy Combust Sci 2002;28:477–542. doi:10.1016/S0360-1285(02)00019-9.

42. Konle M, Sattelmayer T. Time scale model for the prediction of the onset of flame flashback driven by combustion induced vortex breakdown. J Eng Gas Turbines Power 2010;132:041503. doi:10.1115/1.4000123.

43. Friedman R, Johnston WC. The wall-quenching of laminar propane flames as a function of pressure, temperature, and air-fuel ratio. J Appl Phys 1950;21:791. doi:10.1063/1.1699760.

44. Bellenoue M, Kageyama T, Labuda SA, Sotton J. Direct measurement of laminar flame quenching distance in a closed vessel. Exp Therm Fluid Sci 2003;27:323–31. doi:10.1016/S08941777(02)00304-7.

45. Boust B, Sotton J, Labuda SA, Bellenoue M. A thermal formulation for single-wall quenching of transient laminar flames. Combust Flame 2007;149:286–94. doi:10.1016/j.combustflame.2006.12.019.

46. Lewis B, von Elbe G. Stability and structure of burner flames. J Chem Phys 1943;11:75. doi:10.1063/1.1723808.

47. Von Elbe G, Mentser M. Further Studies of the Structure and Stability of Burner Flames. J Chem Phys 1945;13:89. doi:10.1063/1.1724004.

48. Garside JE, Forsyth JS, Townend DTA. The stability of burner flames. J Inst Fuel 1945;18:175–85.

49. Edse R. Studies on burner flames of hydrogen-oxygen mixtures at high pressures. Wright Air Dev Cent Tech Rep 52-59, 1952.

50. Grumer J, Harris MEM. Temperature dependence of stability limits of burner flames. Ind Eng Chem 1954;46:2424–30.

51. Bollinger LE, Edse R. Effect of burner-tip temperature on flash back of turbulent hydrogen-oxygen flames. Ind Eng Chem 1956;48:802–7. doi:10.1021/ie50556a040.

52. Lee ST, T'ien JS. A numerical analysis of flame flashback in a premixed laminar system. Combust Flame 1982;48:273–85. doi:10.1016/0010-2180(82)90134-1.

53. Dugger GLG. Flame stability of preheated propane-air mixtures. Ind Eng Chem 1955;47:109–14. doi:10.1021/ie50541a038.

54. Lewis B, von Elbe G. Combustion, Flames and Explosives of Gases. Third Edit. Academic Press; 1987.

55. White FM, Corfield I. Viscous fluid flow. vol. 3. McGraw-Hill New York; 2006.

56. Harris ME, Grumer J, von Elbe G, Lewis B. Burning velocities, quenching, and stability data on nonturbulent flames of methane and propane with oxygen and nitrogen: Application of theory of ignition, quenching, and stabilizationto flames of propane and air. Symp Combust Flame, Explos Phenom 1948;3:80–9. doi:10.1016/S1062-2896(49)80010-9.

57. Wohl K, Kapp NM, Gazley C. The stability of open flames. Symp Combust Flame, Explos Phenom 1948;3:3–21. doi:10.1016/S1062-2896(49)80005-5.

58. Grumer J, Harris ME. Flame-stability limits of methane, hydrogen, and carbon monoxide mixtures. Ind Eng Chem 1952;44:1547–53. doi:10.1021/ie50511a023.

Wohl K. Quenching, flash-back, blow-off-theory and experiment. Symp Combust 1953;4:68–89. doi:10.1016/S0082-0784(53)80011-1.

59. Grumer J, Harris ME, Schultz H. Flame–stability limits of ethylene, propane, methane, hydrogen, and nitrogen mixtures. Ind Eng Chem 1955;47:1760–7. doi:10.1021/ie50549a024.

60. Berlad AL, Potter AE. Relation of boundary velocity gradient for flash-back to burning velocity and quenching distance. Combust Flame 1957;1:127–8. doi:10.1016/0010-2180(57)90040-8.

61. Fine B. The flashback of laminar and turbulent burner flames at reduced pressure. Combust Flame 1958;2:253–66. doi:10.1016/0010-2180(58)90046-4.

62. Grumer J. Flashback and blow off limits of unpiloted turbulent flames. Jet Propuls 1958;28:756–759.

63. Yamazaki K, Tsuji H. An experimental investigation on the stability of turbulent burner flames. Symp Combust 1961;8:543–53. doi:10.1016/S0082-0784(06)80545-X.

64. Khitrin LN, Moin PB, Smirnov DB, Shevchuk VU. Peculiarities of laminar- and turbulent-flame flashbacks. Symp Combust 1965;10:1285–91. doi:10.1016/S0082-0784(65)80263-6.

65. France DH. Flashback of laminar monoport burner flames. J Inst Fuel 1977;50:147–52.

66. Putnam AA, Ball DA, Levy A. Effect of fuel composition on relation of burning velocity to product of quenching distance and flashback velocity gradient. vol. 37. 1980. doi:10.1016/00102180(80)90085-1.

67. Kalantari A, Sullivan-Lewis E, McDonell V. Flashback Propensity of Turbulent Hydrogen–Air Jet Flames at Gas Turbine Premixer Conditions. J Eng Gas Turbines Power 2016;138:061506. doi:10.1115/1.4031761.

68. Green KA, Agnew JT. Quenching distances of propane-air flames in a constant-volume bomb. Combust Flame 1970;15:189–91. doi:10.1016/0010-2180(70)90030-1.

69. Kim KT, Lee DH, Kwon S. Effects of thermal and chemical surface–flame interaction on flame quenching. Combust Flame 2006;146:19–28. doi:10.1016/j.combustflame.2006.04.012.

70. Friedman R, Johnston WC. Pressure dependence of quenching distance of normal heptane, isooctane, benzene, and ethyl ether flames. J Chem Phys 1952;20:919. doi:10.1063/1.1700600.

71. Potter, A E J, Berlad AI. A thermal equation for flame quenching. NACA TN 1264, 1956:287–93.

72. Ferguson CR, Keck JC. On laminar flame quenching and its application to spark ignition engines. Combust Flame 1977;28:197–205. doi:10.1016/0010-2180(77)90025-6.

73. Potter AE, Berlad AL. The effect of fuel type and pressure on flame quenching. Symp Combust 1957;6:27–36. doi:10.1016/S0082-0784(57)80009-5.

74. Berlad AL, Potter AE. Prediction of the quenching effect of various surface geometries. Symp Combust 1955;5:728–35. doi:10.1016/S0082-0784(55)80100-2.

75. Enomoto M. Head-on quenching of a premixed flame on the single wall surface. JSME Int J Ser B 2001;44:624–33. doi:10.1299/jsmeb.44.624.

76. Popp P, Baum M. Analysis of wall heat fluxes, reaction mechanisms, and unburnt hydrocarbons during the head-on quenching of a laminar methane flame. Combust Flame 1997;108:327–48. doi:10.1016/S0010-2180(96)00144-7.

77. Sotton J, Boust B, Labuda SA, Bellenoue M. Head-on quenching of transient laminar flame: heat flux and quenching distance measurements. Combust Sci Technol 2005;177:1305–22. doi:10.1080/00102200590950485.

78. Dabireau F, Cuenot B, Vermorel O, Poinsot T. Interaction of flames of H2 + O2 with inert walls. Combust Flame 2003;135:123–33. doi:10.1016/S0010-2180(03)00154-8.

79. Enomoto M. Sidewall quenching of laminar premixed flames propagating along the single wall surface. Proc Combust Inst 2002;29:781–7. doi:10.1016/S1540-7489(02)80100-6.

80. Poinsot TJ, Haworth DC, Bruneaux G. Direct simulation and modeling of flame-wall interaction for premixed turbulent combustion. Combust Flame 1993;95:118–32. doi:10.1016/00102180(93)90056-9.

81. Gruber A, Sankaran R, Hawkes ER, Chen JH. Turbulent flame–wall interaction: a direct numerical simulation study. J Fluid Mech 2010;658:5–32. doi:10.1017/S0022112010001278.

82. Veynante D, Vervisch L. Turbulent combustion modeling. Prog Energy Combust Sci 2002;28:193–266. doi:10.1016/S0360-1285(01)00017-X.

83. Clavin P. Dynamic behavior of premixed flame fronts in laminar and turbulent flows. Prog Energy Combust Sci 1985;11:1–59. doi:10.1016/0360-1285(85)90012-7.

84. Haworth DC, Poinsot TJ. Numerical simulations of Lewis number effects in turbulent premixed flames. J Fluid Mech 1992;244:405. doi:10.1017/S0022112092003124.

85. Chen JB, Im HG. Stretch effects on the burning velocity of turbulent premixed hydrogen/air flames. Proc Combust Inst 2000;28:211–8. doi:10.1016/S0082-0784(00)80213-1.

86. Bell JB, Cheng RK, Day MS, Shepherd IG. Numerical simulation of Lewis number effects on lean premixed turbulent flames. Proc Combust Inst 2007;31:1309–17. doi:10.1016/j.proci.2006.07.216.

87. Dinkelacker F, Manickam B, Muppala SPR. Modelling and simulation of lean premixed turbulent methane/hydrogen/air flames with an effective Lewis number approach. Combust Flame 2011;158:1742–9. doi:10.1016/j.combustflame.2010.12.003.

88. Muppala SPR, Nakahara M, Aluri NK, Kido H, Wen JX, Papalexandris MV. Experimental and analytical investigation of the turbulent burning velocity of two-component fuel mixtures of hydrogen, methane and propane. Int J Hydrogen Energy 2009;34:9258–65. doi:10.1016/j.ijhydene.2009.09.036.

89. Bouvet N, Halter F, Chauveau C, Yoon Y. On the effective Lewis number formulations for lean hydrogen/hydrocarbon/air mixtures. Int J Hydrogen Energy 2013;38:5949–60. doi:10.1016/j.ijhydene.2013.02.098.

90. Natarajan J, Lieuwen T, Seitzman J. Laminar flame speeds of H2/CO mixtures: Effect of CO2 dilution, preheat temperature, and pressure. Combust Flame 2007;151:104–19. doi:10.1016/j.combustflame.2007.05.003.

91. Kalantari A, McDonell V. Boundary layer flashback of non-swirling premixed flames: Mechanisms, fundamental research, and recent advances. Prog Energy Combust Sci 2017;61:249–92. doi:10.1016/j.pecs.2017.03.001.

92. Kalantari A, Sullivan-Lewis E, McDonell V. Development of Criteria for Flashback Propensity in Jet Flames for High Hydrogen Content and Natural Gas Type Fuels. US Dep Energy, Final Rep 2016. doi:10.2172/1357931.

93. Akbari A, McDonell V, Samuelsen S. Statistical Evaluation of Rans Simulations Compared To Experiments for A Model Premixer. Eng Appl Comput Fluid Mech 2013;7:103–15. doi:10.1080/19942060.2013.11015457.

94. Kedia, K. S., and Ghoniem, A. F., 2012, “Mechanisms of Stabilization and Blowoff of a Premixed Flame Downstream of a Heat-Conducting Perforated Plate,” Combust. Flame, 159(3), pp. 1055–1069.

95. Lin Y-C, Daniele S, Jansohn P, Boulouchos K. Turbulent Flame Speed as an Indicator for Flashback Propensity of Hydrogen-Rich Fuel Gases. J Eng Gas Turbines Power 2013;135:111503. doi:10.1115/1.4025068.

96. Kalantari A, Auwaijan N, McDonell V. Boundary layer flashback prediction for turbulent premixed jet flames: comparison of two models (2019).

97. Driscoll JF. Turbulent premixed combustion: Flamelet structure and its effect on turbulent burning velocities. Prog Energy Combust Sci 2008;34:91–134. doi:10.1016/j.pecs.2007.04.002

98. Bédat B, Cheng RK (1995) Experimental study of premixed flames in intense isotropic turbulence. Combust Flame 100(3):485–494

99. B.D. Videto, D.A. Santavicca, Combust. Sci. Technol., 76 (1991), pp. 159-164

100. Marshall, A., Venkateswaran, P., Noble, D. et al. "Development and characterization of a variable turbulence generation system," Experiments in Fluids (2011) 51: 611. https://doi.org/10.1007/s00348-011-1082-6

101. Steinberg A.M., Driscoll J.F., Ceccio S.L., Measurements of turbulent premixed flame dynamics using cinema stereoscopic PIV (2008). Experiments in Fluids. doi: 10.1007/s00348-007-0458-0

102. Cheng, R.K., anf Gouldin F.C. (2004). Experimental database for premixed turbulent flames. International Workshop on Premixed Turbulent Flames. http://eetd.lbl.gov/aet/ combustion/workshop/database/flame-config.html.

103. Hultmark M, Bailey SC, Smits AJ. Scaling of near-wall turbulence in pipe flow. J Fluid Mech 2010; 649:103. doi:10.1017/S0022112009994071.

104. Wu X, Moin P. A direct numerical simulation study on the mean velocity characteristics in turbulent pipe flow. J Fluid Mech 2008;608:81–112. doi:10.1017/S0022112008002085.

105. Laufer J. The structure of turbulence intensity in fully developed pipe flow. 1954, NACA

8. Appendix

TASK: DOEx of Flame Holder Temperature

Use Design Expert® to formulate an equation to approximate the temperature of the flame holder based from experimental data at flashback

Since the bulk of this work focuses on realistic gas turbine conditions it is important to make a correlation that can be looked at so an operator can safely understand flashback before it happens. Correlating tip temperature, for a given material and thickness, with another easily defined parameter can help those in the industry to predict potential issues. When this correlation is made it removes the need of additional equations or correlations that would be affected by the fuel composition. The idea of correlating tip temperature and equivalence ratio is a unique idea that can allow for one to back track the adiabatic flame temperature of a specific fuel composition. Comparing the adiabatic flame temperature of a certain fuel composition and the tip temperature will allow one to predict the onset of flashback before any damage or injury occurs.

8.2 Center Body Temperature Prediction

The factor selections are listed below to conduct the design of experiments.

1) Lewis Number (0-1)
2) Pressure (3-10 atm.)
3) Inlet temperature (400-800°F)
4) Equivalence Ratio (0-0.9)

5) Fuel Composition (0-100 H2, 0-70 CH4, and (0-75 CO) [by volume]
6) Flame Temperature (1300-2500K)

The Ranges are between multiple blends of syngas fuels, inlet temps of 400-700°F, pressures from 3-10atm, and equivalence ratios in the lean regime. The Lewis number is chosen because it shows a strong effect of the fuel composition being used. Hydrogen has a strong mass diffusivity compared to hydrocarbons, thus the Lewis number will capture the amount of hydrogen at the given conditions. The Lewis number in these cases are between 0 and 1 (though mostly below 0.3). The pressures and temperatures were chosen to incorporate both low and higher end operation of some gas turbine condition as well as the capabilities of the test cell used. The equivalence ratio captures the amount of fuel in air compared to its stoichiometric balance. The equivalence ratio used was captured at the point prior to flashback. The equivalence ratio values are less than one because gas turbines operate in the lean regime to reduce unwanted emissions and pollutants. The flame temperature varies depending on fuel composition and equivalence ratio at flashback, thus the span of temperatures is wide but needs to be incorporated because it greatly effects the tip temperature of the center body.

The response will be the tip temperature of the center body as it is an important factor in the correlation to predict flashback as shown below. In real world application it is not feasible to insert a thermocouple through the flow and constantly measure the center body tip temperature as it is interfering with the flow, ads additional cost, and is subject to a short lifetime. This project was chosen as it can help combustion engineers with the move towards hydrogen-based fuels and it is a focus of my thesis and work that I enjoy.

The inlet temperature was captured using a k-type thermocouple at the inlet to the rig from the air flow. It records at an accurate enough rate to capture temperature within a 0.5°F

discrepancy. The pressure is captured by a gauge downstream and a PID controller fluctuates the opening of the valve depending on parameters that need to be reached. The Lewis number is captured using Chemkin® and is known once flashback conditions are obtained.

From a combustion background it is known that flame temperature is a very exponential response and it seems obvious that there is much curvature in the phenomena. Response surface design was used as well as Historical data. Both seemed to produce replicate results, thus response surface was chosen due to combustion intuition.

8.3 Center Body Temperature Prediction Formula

Data were inputted into the software Design Expert. All the values inputted in the software were transformed to a natural log value as combustion knowledge states flame temperature is an exponential phenomena. The figure of the Box-Cox plot is shown below in Figure 30 after the natural log transform was conducted. With the natural log values inputted, the Box-Cox plot recommended that a need for a transformation was not needed based on the variation of the minimum and maximum values. This verifies the best developed model accuracy can be achieved.

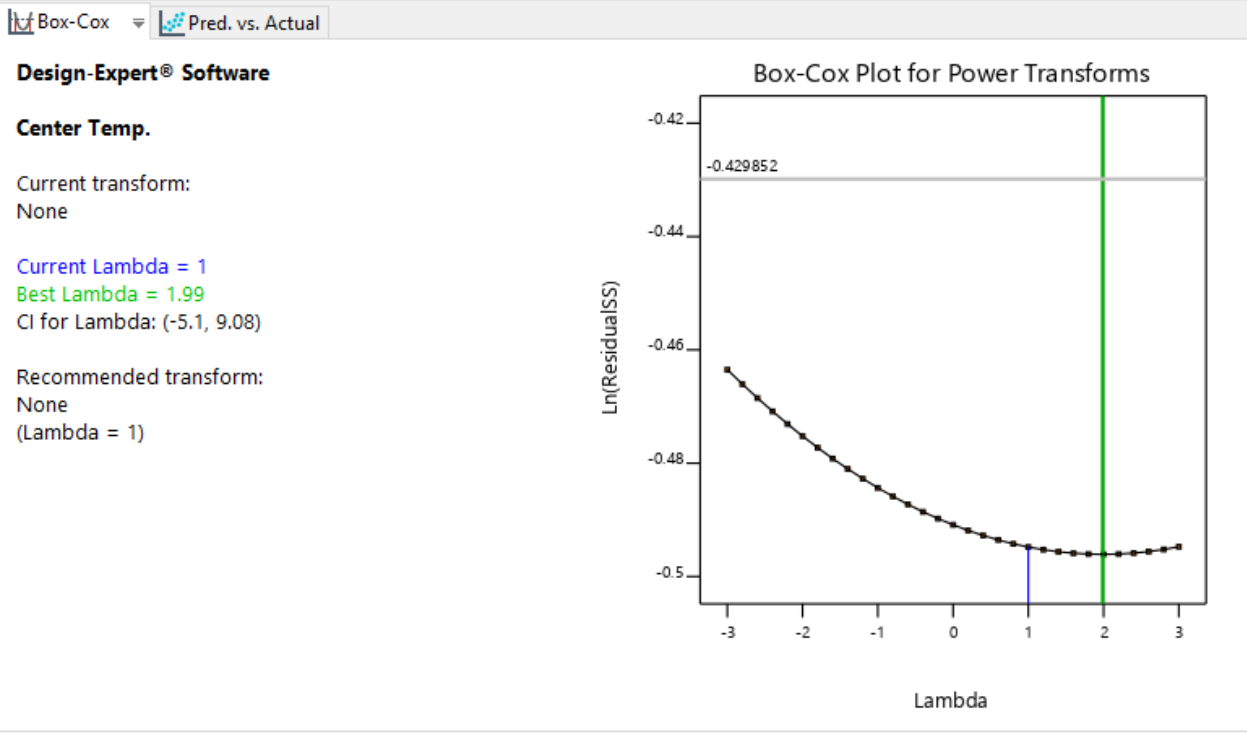

Figure 30: Box-Cox after Ln. Transform Completed

From previous discussion it was mentioned that the model selection process was narrowed down to Historical Data and Response Surface. Both ended up giving same solutions, so the Response Surface was chosen overall since it is known that the phenomena would have curvature.

Multiple iterations were taken to see if the model could be improved. The first included the following factors:

1) Lewis Number (0-1)

2) Pressure (3-10 atm.)

3) Inlet temperature (400-800°F)

4) Flame Temperature (1300-2500K)

This resulted in Resulted in 83.10% Regression, 73.19% Adjusted, and 63.63% Predicted using a reduced Cubic relationship as shown in Figure 31.

Source	Sum of Squares	df	Mean Square	F-value	p-value	
Model	3.00	34	0.0882	8.39	< 0.0001	significant
A-Inlet Temp.	0.0276	1	0.0276	2.63	0.1103	
B-Pressure	0.0540	1	0.0540	5.13	0.0272	
C-Flame Temp.	0.0159	1	0.0159	1.51	0.2235	
D-Lewis #	0.0172	1	0.0172	1.64	0.2055	
AB	0.0103	1	0.0103	0.9793	0.3265	
AC	0.0147	1	0.0147	1.40	0.2420	
AD	0.1001	1	0.1001	9.52	0.0031	
BC	0.0149	1	0.0149	1.41	0.2392	
BD	0.0655	1	0.0655	6.23	0.0154	
CD	0.0293	1	0.0293	2.78	0.1006	
A^2	0.0446	1	0.0446	4.25	0.0438	
B^2	0.0005	1	0.0005	0.0435	0.8355	
C^2	0.0266	1	0.0266	2.53	0.1171	
D^2	0.0310	1	0.0310	2.95	0.0911	
ABC	0.0020	1	0.0020	0.1924	0.6625	
ABD	0.0122	1	0.0122	1.16	0.2852	
ACD	0.0044	1	0.0044	0.4222	0.5184	
BCD	0.0001	1	0.0001	0.0062	0.9377	
A^2B	0.0045	1	0.0045	0.4306	0.5143	
A^2C	0.0077	1	0.0077	0.7352	0.3947	
A^2D	0.0657	1	0.0657	6.25	0.0152	
AB^2	0.0082	1	0.0082	0.7778	0.3814	
AC^2	0.0013	1	0.0013	0.1266	0.7233	
AD^2	0.1254	1	0.1254	11.93	0.0010	
B^2C	0.0049	1	0.0049	0.4666	0.4973	
B^2D	0.0017	1	0.0017	0.1590	0.6915	
BC^2	0.0007	1	0.0007	0.0671	0.7966	
BD^2	0.0256	1	0.0256	2.43	0.1243	
C^2D	0.0090	1	0.0090	0.8602	0.3575	
CD^2	0.0087	1	0.0087	0.8321	0.3654	
A^3	0.0048	1	0.0048	0.4577	0.5014	
B^3	0.0047	1	0.0047	0.4444	0.5077	
C^3	0.0289	1	0.0289	2.75	0.1029	
D^3	0.0114	1	0.0114	1.09	0.3018	
Residual	0.6097	58	0.0105			
Cor Total	3.61	92				

Std. Dev.	0.1025		**R^2**	0.8310
Mean	6.56		**Adjusted R^2**	0.7319
C.V. %	1.56		**Predicted R^2**	0.6363
			Adeq Precision	14.9019

Figure 31: Initial Design Expert ANOVA

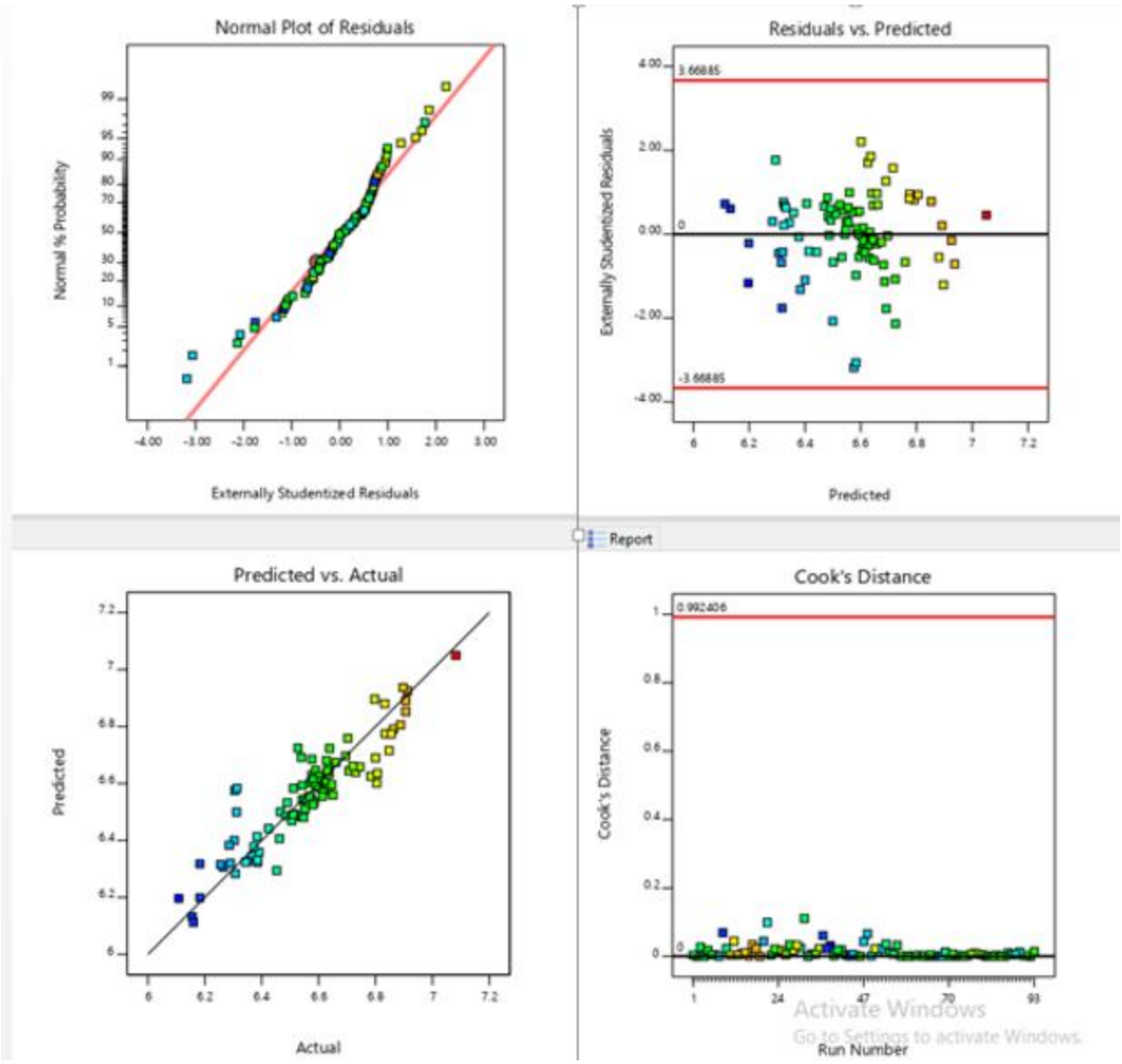

Figure 32: Diagnostics of Initial Results

As it can be seen, the F-values were not great compared to the P values, though the model was significant, it could be better. When it came to the diagnostics it is seen that the normal plot of the residuals lined up nicely as well as the randomness of the Studentized Residuals vs Predicted with no outliers. An undesirable aspect of this initial run was that the equation for the response included many variables as can be seen in the comparison in Figure 35.

The second attempt that was taken was to use the same setup as before but to use an R^2 reduction model to eliminate some variables. The results are shown below in Figure 33.

Source	Sum of Squares	df	Mean Square	F-value	p-value	
Model	2.91	21	0.1386	14.11	< 0.0001	significant
A-Inlet Temp.	0.4318	1	0.4318	43.97	< 0.0001	
B-Pressure	0.3365	1	0.3365	34.27	< 0.0001	
C-Flame Temp.	0.0002	1	0.0002	0.0196	0.8890	
D-Lewis #	0.0033	1	0.0033	0.3339	0.5652	
AB	0.0342	1	0.0342	3.48	0.0662	
AC	0.1630	1	0.1630	16.60	0.0001	
AD	0.6997	1	0.6997	71.26	< 0.0001	
BC	0.2345	1	0.2345	23.88	< 0.0001	
BD	0.6951	1	0.6951	70.79	< 0.0001	
CD	0.1310	1	0.1310	13.34	0.0005	
A^2	0.4051	1	0.4051	41.26	< 0.0001	
B^2	0.0411	1	0.0411	4.19	0.0445	
C^2	0.2126	1	0.2126	21.65	< 0.0001	
D^2	0.0766	1	0.0766	7.80	0.0067	
ABC	0.0915	1	0.0915	9.31	0.0032	
ACD	0.1215	1	0.1215	12.37	0.0008	
A^2D	0.1392	1	0.1392	14.17	0.0003	
AD^2	0.6878	1	0.6878	70.04	< 0.0001	
B^2C	0.0331	1	0.0331	3.37	0.0704	
BD^2	0.5660	1	0.5660	57.64	< 0.0001	
C^3	0.3687	1	0.3687	37.55	< 0.0001	
Residual	0.6972	71	0.0098			
Cor Total	3.61	92				

Std. Dev.	0.0991		**R^2**	0.8067
Mean	6.56		**Adjusted R^2**	0.7496
C.V. %	1.51		**Predicted R^2**	0.7222
			Adeq Precision	18.7553

Figure 33: R^2 Reduction ANOVA

The F-values here increased to be more significant and the p-values remained low, but it still seemed that the flame temperature and Lewis number were not that significant to the model. Though the R^2 value decreased slightly the adjusted and predicted R^2 values became better once some of the unwanted factors were filtered. The diagnostics are shown below in Figure 34.

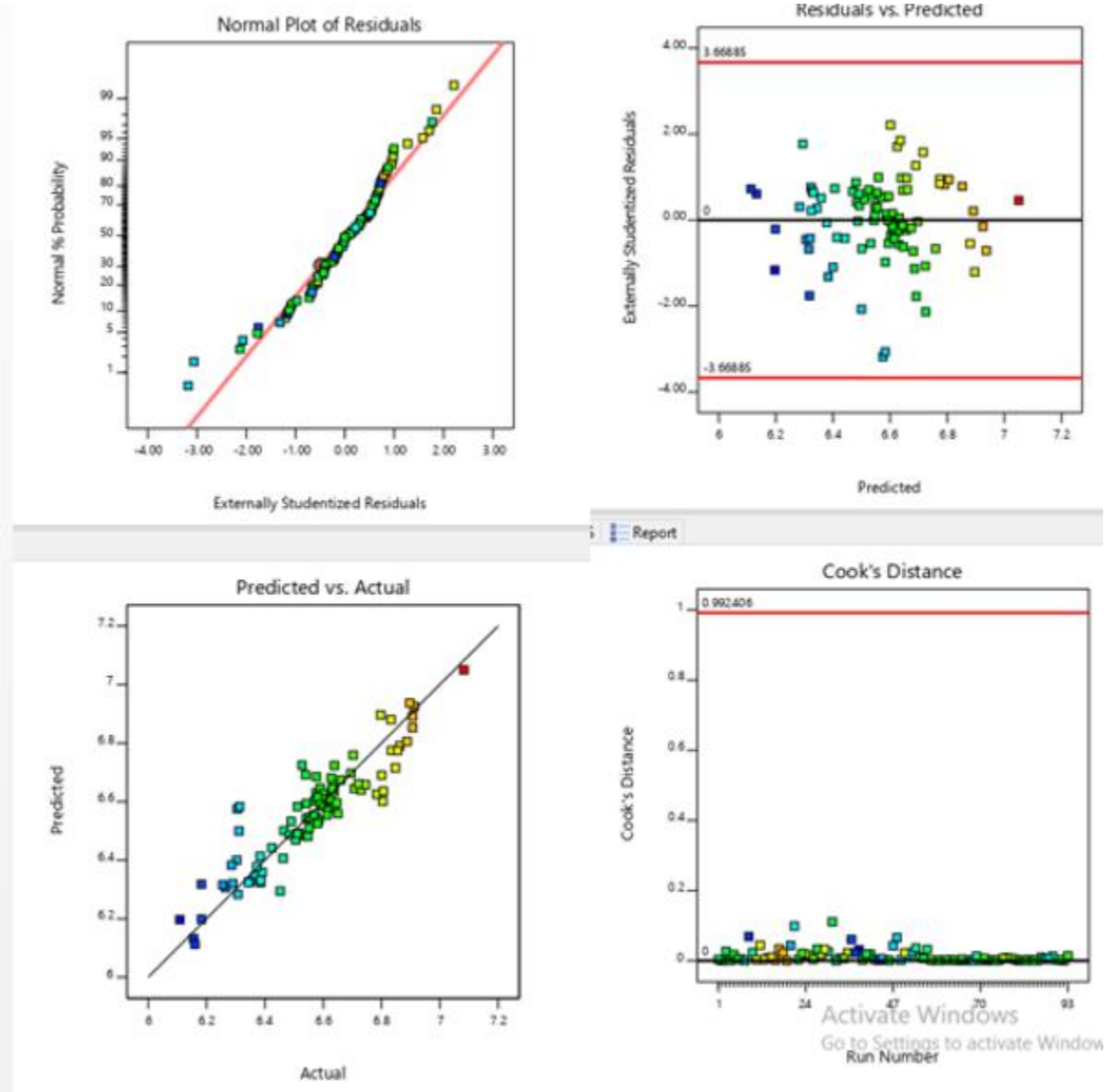

Figure 34: Diagnostics of R^2 Reduction

Comparing the two diagnostics tab we see there is not much visual difference. The equation for the response is now shown and it can be seen apparent that it is more favorable in Figure 35.

Center Temp.	=
-32924.04239	
+1770.80644	* Inlet Temp.
+496.33656	* Pressure
+10678.69517	* Flame Temp.
-3618.42096	* Lewis #
-59.99234	* Inlet Temp. * Pressure
+12.42916	* Inlet Temp. * Flame Temp.
+153.25320	* Inlet Temp. * Lewis #
-102.71554	* Pressure * Flame Temp.
-70.18754	* Pressure * Lewis #
+802.02807	* Flame Temp. * Lewis #
-266.38167	* Inlet Temp.^{2}
+49.02378	* Pressure^2
-1315.65861	* Flame Temp.^{2}
-31.27418	* Lewis #^{2}
+6.00030	* Inlet Temp. * Pressure * Flame Temp.
+20.89860	* Inlet Temp. * Pressure * Lewis #
+29.17633	* Inlet Temp. * Flame Temp. * Lewis #
-2.39490	* Pressure * Flame Temp. * Lewis #
+3.40756	* Inlet Temp.^{2} * Pressure
+15.31530	* Inlet Temp.^{2} * Flame Temp.
-40.52395	* Inlet Temp.^{2} * Lewis #
-3.55827	* Inlet Temp. * Pressure^2
-12.32089	* Inlet Temp. * Flame Temp.^{2}
-60.42451	* Inlet Temp. * Lewis #^{2}
-4.96299	* Pressure^2 * Flame Temp.
-2.39916	* Pressure^2 * Lewis #
+4.77720	* Pressure * Flame Temp.^{2}
+20.21887	* Pressure * Lewis #^{2}
-57.92516	* Flame Temp.^{2} * Lewis #
+43.32407	* Flame Temp. * Lewis #^{2}
+5.52507	* Inlet Temp.^{3}
+1.92702	* Pressure^3
+56.98174	* Flame Temp.^{3}
-16.37915	* Lewis #^{3}

W/O Reduction

Center Temp.	=
-17199.40045	
+160.78190	* Inlet Temp.
+659.88686	* Pressure
+6397.18931	* Flame Temp.
+1228.76958	* Lewis #
-106.01158	* Inlet Temp. * Pressure
+4.13937	* Inlet Temp. * Flame Temp.
-112.63340	* Inlet Temp. * Lewis #
-84.12633	* Pressure * Flame Temp.
+23.71495	* Pressure * Lewis #
-186.07706	* Flame Temp. * Lewis #
-17.73638	* Inlet Temp.^{2}
+20.55586	* Pressure^2
-815.76228	* Flame Temp.^{2}
+251.39448	* Lewis #^{2}
+13.75763	* Inlet Temp. * Pressure * Flame Temp.
+30.97483	* Inlet Temp. * Flame Temp. * Lewis #
-15.96028	* Inlet Temp.^{2} * Lewis #
-43.76666	* Inlet Temp. * Lewis #^{2}
-2.69691	* Pressure^2 * Flame Temp.
+12.49548	* Pressure * Lewis #^{2}
+34.57390	* Flame Temp.^{3}

W/ Reduction

Figure 35: Comparison of Response Equation with and without R^2 Reduction

The last approach taken was to change the Lewis number with an easier determined parameter, the equivalence ratio. The factors chosen for the final attempt is seen below:

1) Pressure (3-10 atm.)

2) Inlet temperature (400-800°F)

3) Equivalence Ratio (0-0.9) [Easier to Know Than Lewis Number]

4) Flame Temperature (1300-2500K)

The results were not as significant as the previous. This was determined mainly from the adjusted and predicted R^2 values having a greater difference that exceeds the software recommendation of 0.2. The ANOVA characteristics can be seen in Figure 36.

Source	Sum of Squares	df	Mean Square	F-value	p-value	
Model	5.871E-06	34	1.727E-07	6.02	< 0.0001	significant
A-Inlet Temp.	3.394E-08	1	3.394E-08	1.18	0.2814	
B-Pressure	7.351E-08	1	7.351E-08	2.56	0.1151	
C-Eq. Ratio	6.132E-10	1	6.132E-10	0.0214	0.8843	
D-Flame Temp.	1.586E-10	1	1.586E-10	0.0055	0.9410	
AB	1.010E-07	1	1.010E-07	3.52	0.0659	
AC	4.138E-08	1	4.138E-08	1.44	0.2348	
AD	3.380E-08	1	3.380E-08	1.18	0.2824	
BC	7.748E-08	1	7.748E-08	2.70	0.1060	
BD	7.496E-08	1	7.496E-08	2.61	0.1117	
CD	9.750E-10	1	9.750E-10	0.0340	0.8544	
A^2	9.105E-08	1	9.105E-08	3.17	0.0803	
B^2	6.034E-08	1	6.034E-08	2.10	0.1526	
C^2	2.078E-09	1	2.078E-09	0.0724	0.7888	
D^2	3.485E-10	1	3.485E-10	0.0122	0.9126	
ABC	1.030E-07	1	1.030E-07	3.59	0.0634	
ABD	9.999E-08	1	9.999E-08	3.49	0.0672	
ACD	4.142E-08	1	4.142E-08	1.44	0.2346	
BCD	7.719E-08	1	7.719E-08	2.69	0.1066	
A^2B	4.298E-08	1	4.298E-08	1.50	0.2261	
A^2C	9.464E-08	1	9.464E-08	3.30	0.0747	
A^2D	8.546E-08	1	8.546E-08	2.98	0.0899	
AB^2	6.886E-08	1	6.886E-08	2.40	0.1270	
AC^2	4.983E-08	1	4.983E-08	1.74	0.1929	
AD^2	3.405E-08	1	3.405E-08	1.19	0.2807	
B^2C	6.991E-08	1	6.991E-08	2.44	0.1242	
B^2D	6.478E-08	1	6.478E-08	2.26	0.1386	
BC^2	8.100E-08	1	8.100E-08	2.82	0.0985	
BD^2	7.449E-08	1	7.449E-08	2.60	0.1128	
C^2D	2.794E-09	1	2.794E-09	0.0974	0.7561	
CD^2	1.481E-09	1	1.481E-09	0.0516	0.8211	
A^3	5.491E-08	1	5.491E-08	1.91	0.1720	
B^3	1.576E-07	1	1.576E-07	5.49	0.0227	
C^3	4.655E-09	1	4.655E-09	0.1623	0.6886	
D^3	6.537E-10	1	6.537E-10	0.0228	0.8806	
Residual	1.577E-06	55	2.868E-08			
Cor Total	7.449E-06	89				

Std. Dev.	0.0002		**R^2**	0.7882
Mean	0.0014		**Adjusted R^2**	0.6573
C.V. %	11.71		**Predicted R^2**	0.4198
			Adeq Precision	13.0625

Figure 36: ANOVA of Equivalence Ratio Attempt

The F-values decreased compared to the last test as well as the p-values got bigger. Replacing the equivalence ratio was not as good as capturing the fuel composition compared to the Lewis number. This can be understood by combustion background. The equivalence ratio is purely a number that does not capture the chemical reactions of the fuel, while the Lewis number can capture the mass vs thermal diffusivity. The Diagnostics are seen below for the iteration including the equivalence ratio in Figure 37.

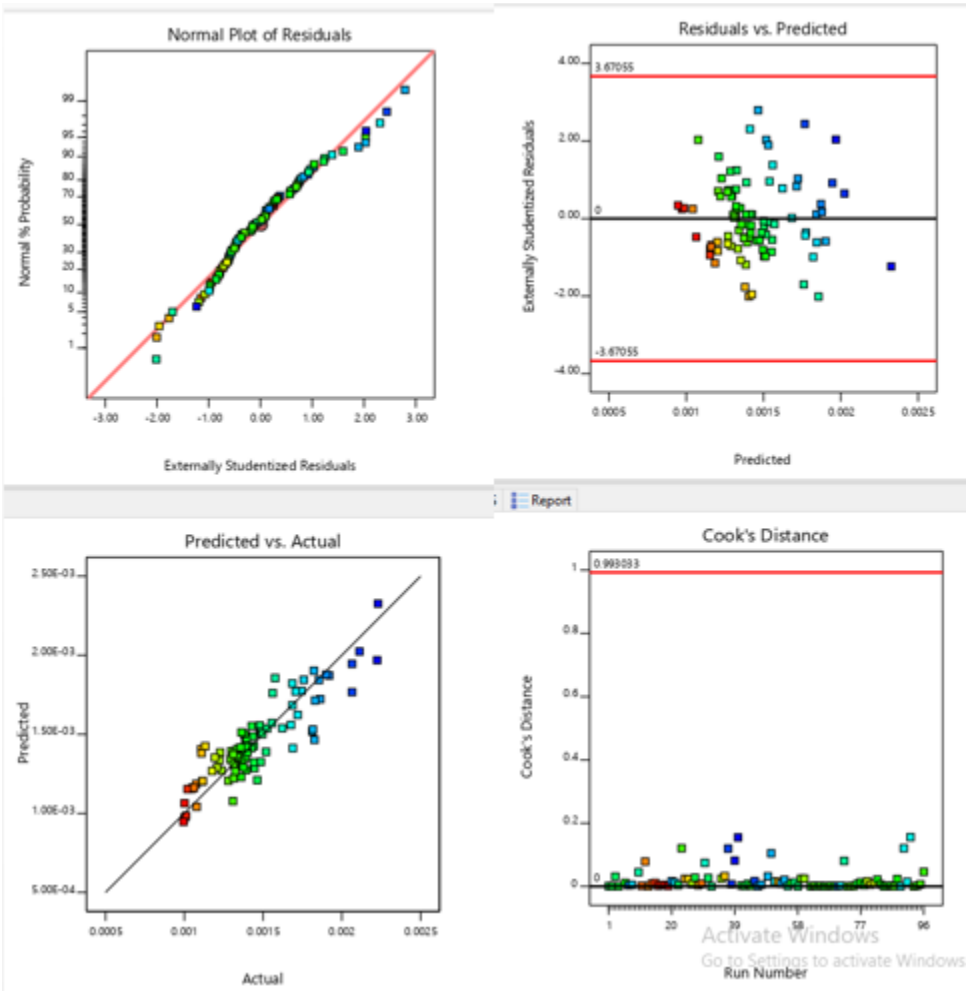

Figure 37: Diagnostics of Equivalence Ratio Run

The final model was chosen to be the R^2 reduction using the Lewis number as a factor instead of the equivalence ratio as it does a better job at capturing fuel affects.

8.4 CONCLUSION/SUMMARY

An equation to estimate the tip temperature of the flame holder at flashback conditions was developed as thermal coupling plays an important role in BLF propensity. The equation was obtained utilizing the Design Expert software. The current work introduces the use of a thermal couple to monitor the barrel tip temperature, which is not applicable in real gas turbine conditions due to additional cost and the short life-span of the thermocouple.

- **An approximate equation to determine flame holder tip temperature was developed to be roughly 81% accurate**

  A cubic relation has been developed to predict the center body temperature based off the factors of the Lewis number, operating temperature, vessel pressure, and flame temperature This modeled equation gives a linear regression of roughly 81%, which is decent for such a complex phenomenon. The operating temperature and pressure are given conditions, though the Lewis number and flame temperature are values that must be calculated. This formula can give insight to predict the center body temperature at flashback conditions, thus allowing the operator to calculate the Da number and find an appropriate velocity to mitigate flashback.

  As thermal coupling plays a significant role in flashback propensity it is important to further develop the equation for better accuracy. The prediction model developed to approximate the tip temperature can further be elaborated on by incorporating a radiation heat loss term from the flame interaction.